Dynamic Topmodel: a new implementation in R and its sensitivity to time and space steps

Peter Metcalfe[1], Keith Beven[1,2] and Jim Freer[3]

[1] Lancaster Environment Centre, Lancaster University, Lancaster, LA1 4YQ UK

[2] Department of Earth Sciences, Uppsala University, Uppsala 75263, Sweden

[3] School of Geography, Bristol University, Bristol BS8 1SS, UK

Abstract

In 2001, Beven and Freer introduced a "dynamic" variant of TOPMODEL that addressed some of the limitations of the original model whilst retaining its computational and parametric efficiency. The original assumption of a quasi-steady water table was replaced by time-dependent kinematic routing within hydrological similar areas. The new formulation allows a more flexible discretisation, variable upslope drainage areas and spatially variable physical properties.

There has, however, never been a freely distributable version of dynamic TOPMODEL. Here, we describe a new, open source, version developed in the R environment. It incorporates handling of geo-referenced spatial data that allows it to integrate with modern GIS. It makes use of data storage and vectorisation features of the language that will allow efficient scaling of the problem domain.

The implementation is evaluated with data from a small catchment. The formulation of the model in terms of a flow distribution matrix is described and its use illustrated for treatment of surface and subsurface flow routing. The model uses an improved implicit solution for updating the subsurface storages and fluxes. The paper focuses on the robustness of the predicted output variables to changes in the time and space discretisations.

Keywords: Dynamic TOPMODEL, R, Gwy, Plynlimon, distributed hydrological model

1 Introduction

Increased computing power, storage and availability of geo-referenced elevation and landscape data has made feasible, in theory at least, the implementation of fully spatial distributed hydrological models. However, in most catchments, the representation of complex fine scale process interactions in heterogeneous flow domains would still quickly overwhelm all but the most powerful hardware. Furthermore, the practical limits on the accuracy and spatio-temporal resolution of catchment data lays open to question whether it could ever contain sufficient information to justify such complex modelling schemes (Beven, 1993, Beven, 2001b, Jakeman and Hornberger, 1993, Beven *et al.*, 2015)

Earlier generations of models were limited, by necessity, to a highly simplified representation of catchment processes. One example is TOPMODEL, a semi-distributed, hydrological model that has been applied in many studies (see Beven, 2012, and references cited therein). Subject to important simplifying assumptions it can simulate the response of a catchment to precipitation falling within the watershed and can also predict the spatial distribution of storage deficits and saturated areas and the initiation of saturation excess overland flow. The principles, assumptions and

mathematics underlying TOPMODEL have been discussed in detail by many authors including Beven and Kirkby (1979); Barling *et al.* (1994); Beven (1997, 2012); Kirkby (1998); and Lane *et al.* (2004) and will not be explained in detail here. The fundamental principle is the aggregation of hydrologically similar areas of the catchment according to the value of a static topographic index. This, combined with a parametrically "parsimonious" approach and straightforward treatment of evapotranspiration and routing, simplifies the computational complexity and allows the model to be run extremely quickly. These properties have allowed the model to be applied in studies of uncertainty estimation requiring many different model realisations and for long simulations for flood frequency estimations (e.g. Cameron *et al.*, 2001; Freer *et al.*, 1997; Blazkova and Beven, 2009).

The "dynamic" extension to TOPMODEL of Beven and Freer (2001) attempted to address the issues arising from the simplified dynamics in the original model whilst retaining its computational and parametric efficiency. In particular, the assumption that the water table could be treated as a succession of steady state configurations consistent with the current subsurface drainage was discarded; instead a kinematic solution was applied to supply a time-dependent solution for the subsurface storage and downslope basal fluxes. The new flow routing and solution procedure for the storage deficits allowed relaxation of the assumption that downslope flows on hillslopes were always connected. It also freed discretisation strategies from the constraint of a single topographic index, and alternative schemes using any hydrologically significant, spatially distributed, characteristics could now be adopted. It also allows a wider spatial application, as the topographic index used by the original model begins to lose physical meaning at resolutions approaching that of global DEMs such as the SRTM and ASTAR GDEM data sets.

Applications of Dynamic TOPMODEL have included defining the parameter distributions needed to predict spatial water table responses (Freer *et al.*, 2004); understanding sub-period seasonally different catchment behaviours (Freer *et al.* 2003); incorporating stream chemistry to understand flux behaviour (Page *et al.*, 2007); the incorporation of different landscape response units to improve spatial conceptualisations (Peters *et al.*, 2003); uncertainty estimation (Liu *et al.*, 2009) and quantifying the effect of spatial rainfall errors on model simulation behaviour (Younger *et al.* 2009).

The introduction of just one new parameter sd_{max} ([L]), allows the model to simulate a variable upslope contributing area due, for example to the breakdown of downslope connectivity (Barling *et al.*, 1994; Jencso *et al.*, 2009; McGuire and McDonnell, 2010). The transmissivity profile is truncated at sd_{max} and when the overall storage deficit for a response unit reaches that level it ceases contributing to downslope flow. This may help to avoid the apparent overestimation of saturated transmissivity to compensate for an overestimation of effective upslope areas in the static topographic index noted by Beven *et al.* (1995) and Beven (1997, 2012).

1.1 Catchment discretisation

Dynamic TOPMODEL implements a formal treatment of the catchment as a "meta-hillslope". Topography, upslope drainage areas and flow distances are important properties of hillslope elements that fix their position and connectivity within this meta-representation (Beven and Freer, 2001). It is still assumed within Dynamic TOPMODEL that areas with similar properties can be grouped together for computational purposes. This reduces run times, always an advantage of the original model, but now allows much more flexibility in defining these Hydrological Response Units (HRUs). In the limiting case where each HRU is identified with an individual raster grid cell this would be equivalent to a fully-spatially kinematic distributed solution at the corresponding grid resolution similar to the DHSVM model

formulation (e.g. Wigmosta and Lettenmaier, 1999). Carefully selected hydrologically significant GIS overlays can be introduced to provide a more detailed discretisation. A hydrological soils classification, such as that produced by Bell (1971) for the Plynlimon research catchments, can be used to inform suitable values for spatially heterogeneous parameters such as porosity and surface conductivity. Geology, vegetation cover and land use could also have a significant impact on hydrological response and spatially-referenced data for these are now widely available, albeit that this is not usually associated with estimates of effective values of the required hydrological parameters. Other spatially derived input data can also be attributed to each HRU allowing for spatial rainfall fields (e.g. Younger *et al.*, 2009) as well as other variables of interest. Therefore the model provides a flexible and powerful modelling framework which allows the user to embed different conceptualisations of hydrological responses within the landscape, thereby maintaining their spatial pattern, and exploring what amount of spatial disaggregation of parameters and structures are needed for individual applications.

Assuming the TOPMODEL kinematic slope-hydraulic gradient approximation, the downslope connectivity can now be inferred from a high –resolution digital elevation model (DEM). This procedure is not constrained to use rectangular gridded data and any method for calculating upslope contributing areas on a digital terrain model could be used (e.g. Tarboton, 1997). Here the M8 multiple flow directional algorithm of Quinn *et al.* (1991) has been used. This uses elevation data in a regular grid and distributes fluxes to all downslope cells, weighted by the slope in each direction. The result is a "flux-distribution" matrix characteristic to a catchment and discretisation that describes the likelihood of flux transfer from elements in one response unit to another. Much of the flux will be redistributed to the same HRU, which is to be expected, as it reflects the downslope transfer of flux through the unit until reaching its boundary with another HRU. This "recycling" proportion will reflect the spatial extent and contiguity of the unit in terms of the probabilities of exchanges between units. These probabilities form the flux distribution matrix within which non-zero elements reflect the positions of the HRU elements in the meta-hillslope..

This matrix, termed $\boldsymbol{W}$ (for weightings), is an important part of the discretisation and programme operation: it maintains information on the connectivity of landscape units in a compact, scale independent structure and is used in the implicit numerical scheme to route subsurface flow between response units. In the new implementation it is also invoked for the routing of surface flow and for model state initialisation. The matrix is constructed by aggregating all the proportions of subsurface flow within each unit, as identified by the M8 algorithm, which flow into other units or reaches of the river network. For n such response units, $\boldsymbol{W}$ is defined as:

$$\boldsymbol{W} = \begin{pmatrix} p_{11} & \cdots & p_{1n} \\ \vdots & \ddots & \vdots \\ & \cdots & \end{pmatrix} \qquad \sum_{i=1}^{n} p_{ij} = 1$$

Element $p_{i,j}$ represents the proportion of flow out of areas in unit i into those of unit j. Given a $n \times 1$ vector $\underline{s_i}$ representing the storage in each HRU at a given time step, $\boldsymbol{W}^T \underline{s_i} dt$ will be a vector whose elements give the total mass flux from all units transferred across the small time interval dt into the corresponding groups.

1.2 Root and unsaturated zone moisture accounting

The representation of unsaturated zone fluxes and evapotranspiration in Dynamic TOPMODEL is straightforward and similar to the original version of TOPMODEL. More complex representations could be included, but Bashford *et al.*

(2002) demonstrated that it was difficult to justify more complex representations of actual evapotranspiration even when "observations" were available at some grid scale above a heterogeneous terrain.

Actual evapotranspiration from each HRU is calculated from the supplied potential evapotranspiration and root zone storage. During dry periods actual evapotranspiration out of unsaturated areas, E_a [L], is calculated using a common formulation that minimises parametric demands (Beven, 2012), and is outlined in the Appendix. Evaporation is removed at the full potential rate from saturated areas and river channels. Rainfall input is added directly to the root zone, and then actual evapotranspiration calculated and removed. If the root zone is filled at this stage any excess rainfall input remaining is added to the unsaturated zone storage. Total drainage into the unsaturated zone across a time step is capped at the amount of remaining storage: overfill is added to the storage excess store and routed overland.

Recharge from the unsaturated zone to the water is at a rate proportional to the ratio of unsaturated zone storage to storage deficit and the gravity drainage time delay parameter, T_d ([T]/[L]). This is equivalent to a time-variable linear store with a residence time per unit of deficit given by T_d (Beven, 2012, Beven and Wood, 1993).

The root zone and interception store is implemented as a lumped store for each HRU. Moisture is added to the root zone store by rainfall input and removed only by evapotranspiration; interaction with the unsaturated zone, for example by capillary uptake, is not considered in this formulation (but see, for example Quinn *et al.*, 1995). Rainfall input is added to each root zone store until "field capacity", the maximum specific storage available $S_{rz,max}$ ([L]), is reached, when it becomes rainfall excess. If storage remains in the unsaturated zone then this is routed to the subsurface, otherwise it contributes to saturated excess flow and routed overland. Fast runoff is generated when the storage deficit in any unit is replenished. This will include both saturation excess runoff and return flows to the surface in areas of convergent topography.

1.3 Subsurface, surface and channel routing

The model assumes that in moderately steep catchments movement in the unsaturated zone is primarily due to gravity drainage to the water table as lateral velocities will be much lower than those in the vertical direction except in steep areas close to saturation. In the 2001 implementation an implicit 4-point time stepping scheme (based on that in Li *et al*, 1975) was implemented to solve the kinematic approximation for the subsurface fluxes. This has been modified in the current implementation to allow for the case where the HRUs are not strictly ordered downslope, as reflected in the general case of $\boldsymbol{W}$ with arbitrary diagonal and off-diagonal elements.

One or more elements of the flux distribution matrix will represent channel reaches and their values represent the proportions of subsurface drainage from each land unit that is transferred to the corresponding river reach. The convention used is for the river units to be held in the initial elements in an order reflecting their downstream positions. The first element of $\boldsymbol{W}$ will therefore generally maintain information for the catchment outlet reach.

A linear network width function routing algorithm, derived from the topography, is used to route channel flow to the outlet (e.g. Kirkby, 1975; Beven, 1979). A fixed channel wave velocity, parameter v_{chan} ([L]/[T]) is assumed with typical values in the range 1000-5000 m/hr. Beven (1979) has shown, based on field evidence, that this is a good approximation for the wave celerity in smaller catchments, even when flow velocities change nonlinearly with discharge. Beven and Wood (1983) demonstrated that hillslope run-off would dominate the hydrograph shape in small

catchments but channel routing would become more significant as the channel travel times start to exceed the model time step. At larger scales, therefore, an improved model could implement a more flexible channel routing procedure that included consideration of network connectivity, bed gradients and other forms of flow depth–discharge relationships.

2 The new implementation

Beven and Freer (2001) implemented the Dynamic TOPMODEL in FORTRAN-77. The code has not previously been publically released, but collaborations were welcome and a number of derivatives developed (e.g Page *et al.*, 2007). In consequence, the model has not been exposed to the range of applications and alternative formulations of the original TOPMODEL. With this goal in mind we have taken advantage of technological, data availability and storage improvements since the original release in order to make available a new, open source version.

Advances since the Dynamic Topmodel was first implemented include:

- software tools for processing of large scale spatial data: in raster and vector formats, for example the Geographic Digital Abstraction Library (GDAL and OGR, www.gdal.org) ,
- widespread availability of desktop GIS software (ArcInfo, SAGA, GRASS, QGIS etc);
- increased availability of geo-referenced data and improvements in bandwidth to allow their electronic delivery;
- availability of storage that allows large quantities of high-resolution digital landscape data to be maintained and computing power for their analysis.

Commercial and open-source GIS now provide extensive scripting capabilities that can be leveraged to provide a programme GUI utilising GIS geo-processing facilities. It was felt, however, that a loosely coupled implementation that utilised data formats compatible with these environments, but that was not dependent on their use, would make the implementation available to the widest audience. This allows users to source and manipulate data in the tool of their choice before supplying it to the model.

2.1 Development environment

We have used the R language and environment (R Core Team, 2013) to develop this new version. R was originally intended as a statistical analysis programming language, but many open-source third party "packages" have extended its capabilities to include time series handling (`zoo`, Zeileis and Grothendieck, 2005; `xts`, Ryan and Ulrich, 2008), spatial analysis (`sp`, Pebesma and Bivand, 2005; `raster`, Hijmans, 2014) and interoperability with GIS and geo-processing libraries (e.g. `spgrass6`, Bivand, 2014; `rgdal`, Bivand *et al.*, 2014). In addition, the environment's origin in statistics and data mining means that it is optimised for integration, analysis and visualisation of large heterogeneous data sets such as those commonly encountered in hydrological analysis (see Andrews *et al.*, 2011). The Python language and MATLAB environments were also considered as a potential implementation platforms, but currently possess relatively basic spatial functionality except through integration with third party GIS software.

The new version of Dynamic TOPMODEL has been implemented as an R package `dynatopmodel` available via the Comprehensive R Archive Network (CRAN) at http://cran.r-project.org/web/packages/dynatopmodel/index.html. The R environment's package system provides a flexible and robust system for delivery and installation of third-party

code. Packages are maintained by CRAN are subjected to rigorous, largely automated, quality-control before being accepted, albeit that this is limited to installation and syntactical correctness rather than algorithmic logic. This, however, may go some way towards giving scientific users the confidence to incorporate external code into their work flow. In addition, under the terms of the CRAN submission policy, documentation, working code examples and source code must be made available. This allows users to both validate the functionality and underlying algorithms of third-party modules and to understand their usage and concepts of the codes.

The R environment is free, open source and multi-platform and provides a useful program development environment for the hydrological researcher. It is intended that other researchers should be able improve, modify and integrate this model with their own work thus the code has thus been structured with readability taking precedence over strict efficiency. As an interpreted language R can have some run time speed issues, such as when many Monte Carlo model runs are required, for example, but the environment can also call executable versions of core programs, as in the R implementation of the original TOPMODEL (see Buytaert *et al*., 2008).

2.2 Landscape pre-processing

A number of R packages for spatial data handling and analysis have been used extensively in the landscape pre-processing routines supplied in the `dynatopmodel` package. R may also integrate with GIS tools such as GRASS through API wrappers, but this would run counter to the "loosely-coupled" approach adopted. Cross-platform file formats such as tiff tagged raster (GeoTIFF) and vector (e.g. ESRI Shapefile) are used, with any non-spatial data maintained as ASCII text.

The `sp` package implements an extremely comprehensive class library for spatial data compatible with the R data structures such as `data.frame` and vector attribute tables maintained in Shape files. Other packages such as `rgeos` (Bivand and Rundel, 2014) and `rgdal` utilise the class hierarchy implemented in `sp` and provide most of the spatial operations found in GIS via interfaces to the GDAL and GEOS geo-processing libraries. The `raster` package inherits from `sp` and, in particular, enables disk-paging of large multi-band rasters such as those used in digital elevation models (DEM) . These are commonly used to maintain gridded catchment elevation data sharing a common extent, resolution and coordinate reference system (CRS). The use of spatially-qualified data significantly improves the geographical and functional range of applicability of the model, allowing landscape layers of different resolutions, extents and CRS to be consistently and quickly integrated and analysed.

Catchment data for a model run comprise a DEM in GeoTiff format and any relevant landscape layers used, and the location of the channel network supplied as a vector Shapefile, with individual reaches and their average widths specified in the `id` and `chan.width` columns of the attribute table. An overall width may be supplied if, as is the default, the river network is treated as a single channel. The procedure and output are illustrated diagrammatically in Figure 1.

Figure 1. Aggregation of landscape layers into a catchment discretisation and its associated data structures

A discretisation strategy is specified by the order and number of breaks to apply to any of the raster layers provided and the chosen definition of the channel network. The routine `disc.catch` provided by `dynatopmodel` generates the files to run a simulation against observation data. This now allows a fast and flexible approach to testing different discretisation strategies and hypotheses regarding the aggregated representations of catchments and landscape layers.

Furthermore, it allows the user to test the results of adding features of an arbitrarily spatial scale that are expected to have a significant impact on the catchment's response. Examples would include impermeable areas that display very fast run-off such as areas of thin soils over granite bedrock found in the Panola catchment study (Peters *et al.*, 2003). Discretisation output comprises:

- A multi-band raster composed of the spatial distribution of the response units followed by the catchment data that were combined to produce the distribution.
- The flow distribution matrix ***W***. Entries in other rows describe, for the HRU represented by that row, the fractional flux out of that unit either to this or another unit or to one of the river reaches.
- Tabulated HRU attributes (see Table 2).
- A channel routing table. This comprises a matrix whose rows represent outlet flow distance distributions, one for each HRU. The columns hold the proportion of the unit's flux that enters the channel at the corresponding distance from the outlet.

Any number of discretisations may be applied to a catchment using `disc.catch` and associated with a single "project" created with `create.proj` (see below). This allows their respective behaviour and performance to be compared and hypotheses regarding the nature and contribution of spatial heterogeneity to be evaluated.

2.3 Data pre-processing and management

Hydrological and meteorological data for run-off models are often of different time ranges and resolution. In addition, spatial data as are required by a semi-distributed model may also vary in extent and resolution and in their coordinate reference systems. Managing these data can become problematic and many software tools have implemented solutions. Some GIS, for instance, have the concept of a geodatabase that can maintain spatial data for a single project.

The `dynatopmodel` package implements a simple project data structure to maintain the heterogeneous data required for analysis of a single catchment. Any number of discretisations applied to a catchment may be associated with a single "project", and , along with rainfall and observed flows, allows their respective behaviour and efficiencies to be easily compared. These facilities are described in more detail in the package documentation for `create.proj`, `add.disc` and related routines, found at http://cran.r-project.org/web/packages/dynatopmodel/dynatopmodel.pdf .A suggested workflow for incorporating existing catchment data and discretisations into a Dynamic TOPMODEL project is given in Figure 2.

Figure 2. Dynamic TOPMODEL pre-processing workflow

Time series input data comprise rainfall, evapotranspiration and any observed discharges. If few meteorological data are available to calculate potential evapotranspiration directly, an additional module `approx.evap.ts` supplied in the can generate a representative time series given a daily maximum and minimum potential evapotranspiration *(E_p)* supplied by the user. This assumes a simple sinusoidal form for daily total insolation across the year and a linear relationship between insolation and E_p. Daily insolation is also assumed to vary sinsuoidally between sunrise and sunset and to integrate to the daily totals.

The routine `run.proj` handles the aggregation and checking of input data maintained in a "project" file created with `create.proj`. Time series are aggregated and averaged to the specified time step and their extents checked for consistency before being supplied to the main simulation routine `dtm.main`.

2.4 Initialisation

The model's behaviour is sensitive to the initial storage and fluxes. The programme allows specification of an initial discharge q_0 ([L]/[T]), assumed to be solely due to subsurface drainage into the river. Determination of the associated storage and unsaturated zone fluxes is then required to prevent a discontinuity in the initial discharges. One approach to would be to run the model for an initialisation period to allow its internal states to stabilise. In the original TOPMODEL this took around 2 weeks of simulation time (Beven *et al*, 1983). It is non-trivial to determine a generally-applicable initialisation period that would ensure that subsurface flows, storages and the river discharge have entirely stabilised by the start of the simulation run. In larger, slower draining and gentle sloped catchments this could be considerable and running for a suitable bedding-in period would affect the run-time performance.

The new implementation instead applies an analytic steady state solution for the specific subsurface flows out of each HRU group, derived by mass balance considerations, and subsurface storages consistent with these discharges calculated by a method outlined in Beven (2012). The procedure is described in more detail in the appendix. The initial state of the catchment is taken as to be a steady configuration where rainfall recharge and unsaturated zone drainage are everywhere equal to the initial specific discharge q_0. Assuming that this results only from subsurface flow, it can be shown that the discharge is related to the average initial storage deficit $\overline{D}$ within each group, which leads to an expression for $\overline{D}$ in terms of q_0. Gravity drainage flux is then initialised to the desired recharge rate q_0, and the corresponding unsaturated storage calculated.

2.5 Subsurface routing

In the earlier version of the model an implicit 4 point numerical scheme was used to solve for the subsurface fluxes out of each response unit over time. This worked correctly if the HRUs are arranged in downslope order, but not when there is potential for interaction between the different grouped HRU elements through the flow distribution matrix. The solution was therefore redesigned, such that the flow distribution matrix incorporated directly into the solution. The new implementation employs a similar approach, but equates the inputs q_{in} into the response units q_{in} with the distribution of base flows q_b by the flux distribution matrix $\boldsymbol{W}$ and unsaturated drainage recharge obtained by the method described in 1.2. This reduces the relationship to a series of differential equations in q_b . The simplified scheme is then solved numerically by the `lsoda` algorithm (Livermore Solver for Ordinary Differential Equations, Petzold and Hindmarsh, 1983) accessed via the `deSolve` package (Seibert *et al.*, 2010). This automatically selects the approach most suitable for the situation encountered: for "non-stiff" systems it employs an explicit predictor-corrector solution, whereas for "stiff" systems an implicit backwards differentiation formula (BDF) is used. Both approaches may be employed during the course of a simulation run. The explicit solution is tried first and the implicit version introduced if the system is found to be substantially non-linear at that simulation time. This approach combines the speed of an explicit approach for periods where flow is fairly stable with the accuracy and stability of an implicit solution when flow is changing rapidly.

2.6 Surface and channel routing

The programme models and reports on overland flow generated by saturation excess, where rain falls on areas that have reach saturation as a result of volume filling from above and from return flow when lateral flux from upper areas exceeds the throughput capacity of downslope areas. Infiltration excess overland flow can also occur when rainfall intensity exceeds the soil's infiltration capacity, but as for the 2001 version, is neglected in the current version in order to avoid introducing additional parameters.

Maximum subsurface flows in each HRU are calculated from the transmissivity profile parameters and limiting transmissivity and local wetness index at each point within the HRU. Flow exceeding this is routed as saturation excess runoff. HRUs are assumed to behave homogenously within their plan area, so that when saturation excess run-off begins anywhere in the HRU it does so across its entire area. This can give markedly different results if the same parameters are applied to groupings of differing resolution (and thus contributing area) or based on different landscape criteria. Sensitivity to the discretisation is tested below.

In the original TOPMODEL, the distribution of the topographic index and model outputs indicate that saturation excess overland flow can often be generated in flatter areas on the hilltops, even though effective contributing areas will be small (Barling, 1994). This will not always be the case. Areas close to the divide with better drainage or larger storage capacities due, say, to thicker soils may remain unsaturated. It is also the case that some or all of the surface flow from upslope might be absorbed, or re-infiltrated, into the "spare" storage capacity of downslope HRUs before reaching the channel. The new version of Dynamic TOPMODEL can handle these types of situation. At each time step, after subsurface fluxes and storages have been updated, surface flow generated in each HRU is added to an excess store for that unit. These are then distributed to downslope areas using the flow distribution matrix and a fixed overland flow velocity for that unit. Depending on the effective surface roughness, overland velocities can range from up to 100 – 200 m/hr (Barling, 1994) to as low as 10 – 30 m/hr (Beven and Kirkby, 1979) through grass and bog vegetation such as sphagnum moss. It is not therefore guaranteed that all surface flow will reach the channel within one time step. The surface excess storages are calculated to the end of the current time interval for all units simultaneously using an implicit scheme. The procedure, described in the appendix, solves a coupled set of differential equations resulting from consideration of the mass balance between input due to redistribution from upslope areas and output through overland flow downslope out of each unit. Overland excess distributed to the channel is routed to the outlet along with subsurface base flow, and updated surface storages in other areas are allocated as rainfall input of the relevant units at the next time step. The excess store is then emptied.

Channel routing is via a fixed wave velocity linear algorithm, as for the original implementation and TOPMODEL. Beven (1979) provides an empirical justification for this approach. Flux transferred to river elements as is aggregated across the inner time steps, and on return to the main loop is routed to the outlet through a time-delay table calculated from the routing table input and the channel wave velocity. An implicit time stepping scheme was implemented using a kinematic wave model but found to have little effect on the results. The modular nature of the code means that swapping out the channel routing logic for a more sophisticated approach based on the Saint-Venant equations, for example, could be used. However, in the test basins considered in Section 14 the linear routing was found to perform well.

2.7 Run time model structure

Input data, such as rainfall, evapotranspiration and those specific to a catchment discretisation, are supplied to the main routine via its arguments shown in Table 1. The entries in Table 1 are supplied as named parameters to the routine `dtm.main` shown at the start of the programme flowchart in Figure 4. A conceptual model of a Hydrological Response Unit within the new implementation, along with linkages with other units and model components is shown in Figure 3. The storages associated with HRU entities are defined in Table 3 and flows (shown by arrows linking entities in Figure 3) in Table 4.

Table 1: Main routine input parameter list

Internal name	Description	Symbol	Units	Default
`groups`	Response unit info (described in Table 2)			
`dt`	Main time step	Δt	*hr*	1
`w`	Flux distribution matrix	$\boldsymbol{W}$		
`rain`	Precipitation times series, at same interval as main time step		*m*	
`pe`	Potential evapotranspiration, at same interval as main time step		*m*	
`qobs`	Observed discharges – will be aggregated to main time step		*m/hr*	
`v.chan`	Channel routing wave velocity	v_{chan}	*m/hr*	3000
`ntt`	Number of inner time steps			4
`routing`	Routing table			

Areal grouping properties, storages and fluxes associated with each HRU are maintained in R data frames, similar to the tables from relational databases. Each row corresponds to a single HRU and each column to the (possibly time-varying) quantities or fixed properties for that area. The vectors corresponding to each column can be referred to by name and operations between them quickly performed element-by-element.

On initialisation external rainfall input is distributed between the groups. The model assumes spatially homogeneous rainfall but allows for spatially distributed input by associating each HRU with a particular rainfall record via the column index of the rain given by the value of `gauge_id` in the `groups` table, shown in Table 2

Table 2: `groups` input table structure

Internal name	Description	Symbol	Units	Default
`id`	HRU ID	-	-	
`gauge_id`	Rain input gauge ID	-	-	1
`area_pc`	Catchment areal contribution of unit		%	-
`area`	Total plan (map) area of unit		m^2	-
`atb_bar`	Average value of *ln(a)/tan(β)*index		m^2/m	-
`sd_max`	Max deficit before subsurface flow ceases	sd_{max}	*m*	0.3
`v_of`	Overland flow velocity within area	v_{of}	*m/hr*	100
`td`	Unsaturated zone drainage delay	t_d	*hr/m*	10
`srz0`	Root zone storage initially occupied	srz_0	%	100
`m`	Recession parameter	*m*	*m*	0.01
`ln_t0`	Saturated transmissivity	$ln(T_0)$	m^2/hr	5
`srz_max`	Maximum root zone storage	srz_{max}	*m*	0.1

The properties and state of each HRU are maintained in `groups` and `stores` data frames, and the internal and external fluxes that link them to other units and the exterior of the catchment by `flows`. The `groups` frame is supplied externally from the results of catchment discretisation, and `stores` and `flows` at each step in the simulation period are calculated and returned by the programme.

Table 3: `stores` internal table structure

Internal name	Description	Symbol	Units
`id`	HRU ID		
`suz`	Unsaturated zone storage	s_{uz}	*m*
`srz`	Root zone storage	s_{rz}	*m*
`ex`	Saturation excess storage	s_{sat}	*m*
`sd`	Saturated storage deficit	s_d	*m*

Table 4: `Flows` internal table structure

Internal name	Description	Symbol	Units
`id`	HRU ID		
`pex`	Precipitation excess draining root zone to unsaturated zone	$p_{ex}p$	*m/hr*
`uz`	Gravity drainage from unsaturated zone into water table	q_{uz}	*m/hr*
`qb`	Specific subsurface downslope flow	q_b	*m/hr*
`qin`	Upslope total input flow	q_{in}	m^3/hr
`qex`	Saturated excess flow	q_{ex}	*m/hr*

Flows and stores map to components of the conceptual response unit shown in Figure 3.

Figure 3. Conceptual structure and interfaces of hydrological response groups. Components map to the fields in tables 1 -3

The module `init.input` validates the input, establishes the required data structures and initialises subsurface fluxes and storages using the approach outlined above. The programme then steps through the simulation period using the

specified time interval `dt`, with the moisture accounting and subsurface routing undertaken in an inner loop. The modular programme structure is illustrated in Figure 4.

Figure 4. Dynamic TOPMODEL modular programme structure

3 Test data

3.1 Artificial landscapes

The basic operation of the model code and the sensitivity of the results to changing space and time discretisations were tested with a simple ”artificial” catchment divided into increasing numbers of downslope classes. The catchment takes the form of a V-shaped valley, with a convergent source area and convexo-concave hillslopes.

Figure 5: Simulated upland basin with a simple straight channel used in initial spatial and temporal sensitivity tests. Results are shown of an aggregation into 5 units according to upslope contributing area. Bar plots shows the plan areal contribution

Rainfall data used were from a representative period from the Gwy catchment that will be described below, but the response to “artificial” rainfall events such as a short, intense impulse event was also examined.

3.2 Gwy test catchment

Data for a well-instrumented upland catchment were used to test the model for its performance against observed discharge data and response to spatial and temporal schemes applied to actual topographic data. The Gwy forms the headwaters of the River Wye in Powys, Wales, draining the highest part of the Plynlimon massif, and has an average elevation of 586m. It is contained within the Plynlimon research catchments established in the late 1960s by the then Institute of Hydrology (now the Centre for Ecology and Hydrology, CEH) in order to investigate the differential uptake of water by forestry and open grassland. It has an area of 3.65 km² divided between a main basin and a southern tributary, the Nant Gerig. Soils are blanket peat on the flat summit areas, peaty pozdols on the hillslopes and gleys in the valley bottoms (Kirby *et al.*, 1991, Newson, 1976b). The highest areas are heath, grassland predominates on the better-drained hillslopes and mires occupy the valley floors. Underlying bedrock is Ordovician massive gritstone whilst higher elevation areas are slates and Silurian mudstones (Newson, 1976b). Precipitation is high, averaging around 2600mm pa, dominated by synoptic rainfall that occurs throughout the year. Peat on south to south-westerly aspects is subject to desiccation which when on slopes steep enough (>0.2) to impart sufficient hydraulic gradient has lead to the formation of intricate networks of near surface “soil pipes” (Newson & Gilman, 1980; Jones, 2010). The catchment has been instrumented since the early 1970s and flows at 15 minute intervals collected at a gauging station established in 1999 just upstream of its confluence with the Nant Iago. The flume is a rectangular, side contracted critical depth design suitable for use in small catchments exhibiting a range of discharges and easy to clear of solids deposited by the heavy sediment loads.

Figure 6: Overview of Gwy test basin, showing its location within the Plynlimon research catchments in mid Wales. The channel network for Wye and weather station locations are also shown. Digital elevation data ©Ordnance Survey (GB), 2012. Catchment boundaries and digital river network, CEH (2012)

Hourly rainfall and a variety of other chemistry and meteorological data have been collected since 1976 from Automatic Weather Stations (AWS) at Carreg Wen and Eisteddfa Gurig, located at about 500m in the upper parts of the Hafren and Cyff subcatchments bounding the Gwy to the north and south, respectively, and at Cefn Brwyn near the catchment outlet. Newson (1976a) noted significant variations across small spatial scales in these catchments, which she attributed mainly to orographic effects. Data for 2008 for the two upper gauges obtained from CEH and displayed good agreement, with a correlation of 0.88, and for this study the rainfall input for Carreg Wen was applied homogeneously across the catchment.

A test period of around 4 months from early 2008 was chosen (Figure 77). Discharge and rain records are continuous across the period and other AWS data show that snow fall was negligible. The period contained both a series of intense rainfall events that took place in the week of the 14th to 21st January when storm flows of up to 7.33 mm/hr were recorded, and an extended recession period in mid-February which saw over a week of discharges < 0.05 mm/hr. The storm events allowed us to test the model's capacity to simulate high flows where saturation excess overland flow becomes significant. Simulation of low flows and the response in wetting-up periods can also be considered during the dry period in February and the subsequent prolonged rainfall. Average time from peak rainfall to discharge in the order of just 1 to 2 hours; in the first storm the discharge is seen to rise within 9 hours from a minimum at the end of a recession period of 2.6 mm/hr to a maximum of 6.9 mm/hr.

Long term studies of the water balance of the area (e.g. Marc and Robinson, 2007) have concluded that the catchments are relatively impermeable with little loss of water through the bedrock. Thus the 0.25m excess of rainfall over discharge observed in 2008 was taken to be solely due to evapotranspiration. This is considerably lower than figures of between 0.435m and 0.491m for the entire Wye catchment (see Marc and Robinson, 2007, and references cited therein). It is, however, consistent with average E_a they quote of 0.255 m/pa for the Gwy in the years 1972-2004. McNeil (1997) gives an estimate for 1992 of 0.91 for the E_a/E_{pp} ratio in the upper areas of the Wye. If this is assumed to be entirely evapotranspiration, the total E_p estimated for the year would be 0.28 m. An hourly time series consistent with this total was generated using the `approx.pe.ts` routine provided in the `dynatopmod` package, specifying a daily maximum potential evapotranspiration of 1.5 mm and minimum of 0.

Figure 7: Test period showing rainfall, estimated potential evapotranspiration (in brown, simulated) and observed discharges at the Gwy flume. Storms occupy the first month of the simulation, separated by a week of dry weather from a period of less intense but persistent rainfall lasting from late February through to April

Discretisations based around the local slope, upslope contributing area and flow distance to the nearest channel (both obtained through the D8 algorithm) were tried. These were considered to most closely correlate with the spatial distribution of the hillslopes and so allow the effect of increasing the numbers of downslope groups to be more easily observed. The upslope area was selected as it is quickest to calculate from within the programme environment and so could be used to investigate the response to spatial discretisation.

The channel network used was derived from aerial survey commissioned for the Plynlimon project (Robinson *et al.*, 2008). Due to the small size of the catchment and relatively high bed gradients most flow entering the channel is likely to pass through the outlet within an hour time step. Although the programme allows for multiple reaches with varying widths, the channel was therefore represented as a single reach of nominal width of 1m throughout; the resulting channel approximation occupied 1.7 % of the catchment area.

4 Results

4.1 Parameter estimation

The emphasis of this paper is on the numerical performance of the model, but for this to be carried out a behavioural parameter set is required. A likely range for the recession parameter m can be estimated from the falling limbs of the hydrograph using the semi-automated technique of Lamb and Beven (1997). The onset of saturated excess overland flow is largely controlled by the limiting transmissivity $ln(T_0)$; the initial rapid response and storm-level discharges appeared to require the initiation of these flows. For example, the peak on the 15th January could best be simulated by allowing two to three hours of saturation overland flow to occur; while in the later storms additional return flow was required to match the peak flows. Manual adjustment of the parameter values and examination of its effect on the flow peak thus allowed a probable range for $ln(T_0)$.to be estimated. Approximately 5000 parameter sets were sampled from the ranges given in Table 5 and a simulation run for each, using a 7.5 minute time interval, across the first series of storm events in the test period. This showed the performance to be most sensitive to the values of $ln(T_0)$ and m but, inside a broad range of values, relatively insensitive to unsaturated drainage delay t_d and initial and maximum root zone storage, srz_{max}; their effect was greatest at the start of the simulation and the onset of flow after a recession period. As these occupy a small proportion of the simulation time their effect on any quantitative measure of model fit is likely to not reflect the effect on the qualitative fit. These latter parameters were therefore fixed at representative values well inside these stable regions. Given that the test period contained no extended dry spells with high evapotranspiration the maximum deficit sd_{max} was not found to be relevant.

Table 5: parameter ranges and values used in response tests

Parameter	Description	Units	Lower	Upper	Applied
v_{of}	Overland flow velocity	m/hr	10	150	100
m	Form of exponential decline in conductivity	m	0.0011	0.033	0.0068
srz_{max}	Max root zone storage	m	0.01	0.2	0.1
srz_0	Initial root zone storage		0.5	1	0.98
v_{chan}	Channel routing velocity	m/hr	500	5000	3000
$ln(T_0)$	Lateral saturated transmissivity	m²/hr	3	16	15.2
sd_{max}	Max effective deficit of saturated zone	m	0.2	0.8	0.5
$1/t_d$	Reciprocal of unsaturated zone time delay	m/hr	0.01 (100)	100 (0.01)	2 (0.5)

The code limits unsaturated zone drainage across a time step to the contents of the zone, meaning that very small values of t_d effectively drain the entire zone within one time step. Corresponding values for time delay are shown in brackets. The parameters identified were then used in the following responses tests.

4.2 Sensitivity of model outputs to temporal discretisation

The kinematic approximation for the subsurface storage, although solved with an implicit solution scheme, is sensitive to non-linearity in the storage-discharge relationship. This leads to a potential loss of accuracy in periods where the response is most non-linear. Numerical inaccuracies that arise due to inappropriately applied time-stepping schemes can even outweigh structural errors within a model (see Clark and Kavetski, 2010). Dynamic TOPMODEL implements an scheme to solve for the subsurface fluxes across time and allows this to be run within an inner loop with an arbitrary number of time steps. The number of steps is set by the parameter `ntt` with a default of 4. This

should reduce numerical dispersion and the potential for non-convergence where non-linearity has greatest impact. Root and unsaturated zones are updated explicitly and here the choice of time step will have greater impact, and these routines are also run within the inner loop. The inner loop enables discharges to be simulated at the same outer time step as observed flows, for example, whilst running internally at a much finer time interval. Surface routing makes use of an implicit approach and channel routing a time delay algorithm, and both are run in the outer loop. A further advantage of using an inner loop is, therefore, that the same channel routing table may be used for a range of inner time steps.

4.2.1 Temporal response - test landscapes

To test the effect of the inner time interval a simulation using 5 response units was run repeatedly, at each stage increasing the numbers of steps. A representative parameter set was used with values taken from the last column of Table 5. Channel routing velocity was 3000 m/hr, which ensured that all flow left the basin within one time step. An outer time interval of 1 hour was used and 1, 2, 4, 8 and 12 inner steps applied, corresponding to intervals of 60, 30, 15, 7.5 and 5 minutes respectively. Responses are summarised in Figure 8 and Table 6.

Figure 8. Response of hypothetical catchment to changes in time interval. Shown are the absolute difference of the predicted discharges within each trial from those predicted using a time step of 5 minutes. Central part of storm event within test period show and evapotranspiration output supressed.

Mean absolute difference of observations between successive trials is given by $\overline{\left|\left(q_{\Delta t_i} - q_{\Delta t_{i-1}}\right)\right|}$. The mean difference of observations between each trial and the trial with the smallest time step is given in the column headed $\overline{\left|\left(q_{\Delta t_i} - q_{\Delta t=5}\right)\right|}$ in Table 6

Table 6: Temporal sensitivity response: $q_{\Delta t_i}$ is the simulated discharge when using the time interval Δt_i .

Δt (min)	**Water balance %**	$\sum \boldsymbol{q_{\Delta t_i}}$ **(m)**	$\overline{\left\|\left(\boldsymbol{q_{\Delta t_i} - q_{\Delta t_{i-1}}}\right)\right\|}$ **%**	$\overline{\left\|\left(\boldsymbol{q_{\Delta t_i} - q_{\Delta t=5}}\right)\right\|}$ **%**
60	1.2	0.62		3.2
30	1.2	0.62	1.7	1.5
15	1.2	0.62	0.88	0.6
7.5	1.2	0.62	0.45	0.15
5	1.2	0.62	0.15	0

Convergence between successive trials and approach towards the final response is seen. As the time interval decreases flood peaks become more pronounced and model response more rapid. Water balances and flow totals are consistent, demonstrating the soundness of the internal operation of the model and its moisture accounting logic. The excess is due to channel and root zone storage that has not been accounted for between the start and end of the runs.

4.2.2 Temporal response - Gwy

Sensitivity tests to time and space intervals were undertaken as for the simulated catchments. A discretisation comprising 8 response units was used with the parameters shown in the final column of Table 5 were applied to all units. The mean percentage difference between observations from consecutive trials is given by $\overline{\left|\left(q_{\Delta t_i} - q_{\Delta t_{i-1}}\right)\right|}$. The mean percentage difference of observations between each trial and the final run, using a 5 minute time interval, is given as $\overline{\left|\left(q_{\Delta t_i} - q_{\Delta t=1}\right)\right|}$ in Table 7. The total discharge through surface saturation flow, $\sum q_{ovf}$, is also recorded.

Table 7: Temporal response for Gwy catchment. Figures to 2 s.f.

Δt (min)	Water balance %	$\sum q_{\Delta t_i}$	$\sum q_{ovf}$ (mm)	$\overline{\lvert(q_{\Delta t_i} - q_{\Delta t_{i-1}})\rvert}$ %	$\overline{\lvert(q_{\Delta t_i} - q_{\Delta t_5})\rvert}$ %
60	0.18	0.62	0.23		2.2
30	0.18	0.62	0.16	1.2	1
15	0.19	0.62	0.12	0.6	0.41
10	0.19	0.62	0.1	0.2	0.2
5	0.19	0.62	0.063	0.2	0

Successive trials steadily approach the results of the final run and the differences between successive runs also decrease in a predictable manner. Overland flow totals decrease with time interval. This may be due to saturation excess flows of duration shorter than the time step, where the entire interval might be identified with the saturated flow leading to an apparent overestimation. Total discharges over the simulation period are constant, however, showing that flow not routed overland is being routed by fast subsurface flow.

4.3 Sensitivity of model outputs to spatial discretisation

The model allows the catchment to be discretised to any level of detail until the limiting case where a single grid cell is identified with a single HRU. Experience with the original TOPMODEL shows, however, that there is likely to be a number above which any improvements in the model's performance is outweighed by performance overheads and the limitations in the observed input and output data (e.g. Beven and Smith, 2014). To test this effect in the new model, a parameter set and time step were fixed and successively finer discretisation based on upslope specific drainage areas applied.

Onset of saturated flow is largely controlled by limiting transmissivity and the overall wetness index. .As the latter increases exponentially with distance downslope, very fine discretisations can lead to areas close to the channel apparently providing overland flow in response to any rainfall. This effect was overcome in the catchment pre-processing by applying a minimum areal contribution of 1% for an area to appear in the discretisation; smaller areas are amalgamated with those adjacent until the threshold is reached.

4.3.1 Spatial response - test landscapes

As for the temporal response analysis, the mean difference of observations between successive trials is given in Table 8 in the column labelled $\overline{|(q_i - q_{i-1})|}$. The mean difference of observations between each trial and the trial with the finest spatial discretisation is again given in the final column. The outer time step was 1 hour with 2 inner steps applied and the parameters as for the temporal response tests.

Table 8: Sensitivity to change in spatial discretisation: 1 to 14 downslope elements (figures to 2 s.f.)

No. groups	Water balance %	$\sum q_i$ (m)	$\overline{\lvert(q_i - q_{i-1})\rvert}$ %	$\overline{\lvert(q_i - q_n)\rvert}$ %
1	1.2	0.61		0.011
2	-1.3	0.62	2.5	2.6
5	0.14	0.62	1.5	1.1
8	0.65	0.61	0.51	0.56
12	1.2	0.61	0.56	0

The responses are plotted in Figure 9.

Figure 9. Response of hypothetical catchment to changes in time interval. Shown are the absolute difference of the predicted discharges within each trial from those predicted using a time step of 5 minutes. Central part of storm event within test period shown and evapotranspiration output suppressed. Observed discharges are shown using the RH axis for scale

The response begins to stabilises above 2 units, with flood peaks becoming progressively more pronounced as the number of units passes 8. The highest peak does appear to decrease after this point, however, and there is also slight increase in the difference between the successive trials. The fluctuations in successive trials may be caused by the variation in size of the unit closest to the channel and the corresponding amount of saturated overflow flow it contributes during storms.

4.3.2 Spatial response - Gwy

Real landscapes are more spatially heterogeneous than the artificial catchment considered and likely to show sensitivity to discretisation. A spatial response analysis was therefore also undertaken for the Gwy. As before, the parameter set from Table 5 was used, a 15 minute outer time step and 2 inner steps applied. The results are presented in Table 9; with the final column giving the mean difference of observations between each trial and that employing the finest spatial discretisation.

Table 9: Sensitivity to changes in spatial discretisation within Gwy catchment, n_{max}=12 units. Figures to 2sf

n	Water balance %	$\sum q_n$ (m)	$\overline{\lvert(q_n - q_{n-1})\rvert}$ %	$\overline{\lvert(q_n - q_{n_{max}})\rvert}$ %
1	0.2	0.63		0.85
3	0.14	0.63	1	0.32
6	0.098	0.63	0.18	0.14
9	0.071	0.63	0.11	0.029
10	-0.084	0.63	0.62	0.6
12	0.064	0.63	0.6	0

The model seems responsive to spatial discretisation only up to a few groupings and it quickly converges towards the final results, although there seem to be some fluctuations in differences between successive trials.

4.4 Testing the Gwy catchment model

The aim of this paper is to present the new implementation of Dynamic TOPMODEL and investigate its numerical consistency. A full model calibration and uncertainty analysis will be presented in due course. However, to illustrate the model performance for the Gwy catchment, Figure 10 shows some detail of the discharge predictions for the 4 month test period described using a 5 minute inner time interval. A high resolution plot for the whole of 2008 is given in the Electronic Supplement to this paper. This gave a good visual fit and a Nash-Sutcliffe Efficiency of 0.88; the NSE for the simulation over the four month calibration period was 0.91.

Figure 10: Four month validation period showing observed discharges (green) and simulated (blue) values for a run using a 15 minute time interval and 3 inner steps. Calculated actual evapotranspiration is shown in brown using the scale on the RH axis.

5 Discussion

Modelling can be seen as a means of mapping a complex physical system to a simplified representation tractable to simulation and hypothesis testing (e.g. Beven 2002b, Clark *et al.*, 2011; Beven *et al.*, 2012). The discretisation process employed by Dynamic TOPMODEL allows aggregation at various scales within the same structure, in the same way that spatial data in vector format allows features of any scale to be represented with minimal storage requirements. Recent years have seen increasing interest in multi-scale and ensemble environment models, and these frameworks recognise that the optimal aggregation of a physical system is dependent on the dominant processes at the scale being considered (see e.g. McDonnell *et al*, 2007). Given sufficiently detailed elevation and river network data, the Dynamic TOPMODEL approach achieves such a simplification up to catchment scale whilst retaining information on hydrological connectivity between hydrological response units and the associated inputs channel network (via the flow distribution matrix). The important aspect of TOPMODEL, that the results from a relatively simplified model structure can still be mapped back into space, is retained, and provides additional information for testing whether a model is acceptable in its representation of runoff processes and deciding whether additional spatial complexity of parameters is justified.

Here we have concentrated on exploring the numerical characteristics of the model. This revealed that while the original implementation of Dynamic TOPMODEL made use of an implicit time stepping scheme for each HRU derived from a kinematic wave analogy, the implementation of this method was not fully implicit because the flows from "upslope" were only estimated at the start of the iteration. This has been corrected in the new implementation, however, explicit schemes for root and unsaturated zone moisture accounting remain and may be improved in the future. Thus the tests in this paper show that the predicted discharges are sensitive to both the time and space discretisations, but converge as the internal time step is reduced and the number of downslope HRUs increase. This concurs with Clark and Kavetskis' (2010) conclusion that the use of coarse time resolutions and spatial discretisations will have an impact on the parameter values required for the model to give an acceptable fit to observations.

Further work will also be required to develop a version with run times fast enough to be used effectively within hypothesis testing approaches. It is also currently inadequate for calibration and uncertainty estimation, or for evaluation over longer time periods. The ability to run the kinematic solution within in an inner time stepping loop may, however, allow an adaptive scheme that could improve the model's performance. The inner time period would be decreased in period of high subsurface flow and low deficit when the model sometimes appears to require a shorter interval to fully capture the dynamics of storm flows. An improved treatment of the unsaturated zone, as suggested by Beven and Freer (2001), may further improve performance. Explicit schemes for root and unsaturated zone moisture accounting make these more sensitive to the time interval: in the response tests a stable response appeared as the time interval was decreased; below this no further change in the response could be seen. In the test catchment the critical time interval appears to be around 5 minutes, but is likely to be catchment-specific and longer for less responsive areas.

The more CPU intensive routines could be delivered as compiled modules written in C++ or FORTRAN, as was done by Buytaert (2011) in his implementation of TOPMODEL, although this might reduce the flexibility and portability of the implementation. The R byte code compiler (R Core Team, 2013) may also be able to reduce run-times. Use too

could be made of matrices rather than data frames, albeit with a potential loss of readability, and pre-compiled libraries for efficient manipulation of data structures.

The size and resolution of the discretisation used seemed to have little impact on run times, and beyond about 5 – 8 units a surprisingly small impact on the model response. In larger catchments more numerous HRUs may be required to adequately represent spatial heterogeneity, and repeated multiplication by the flow distribution matrix $\boldsymbol{W}$ is likely to have performance effects. Operations on sparse matrices such as $\boldsymbol{W}$ would be handled much more efficiently by making use of the `spam` package (Furrer and Sain, 2011).

6 Conclusions and further developments

This paper has described the new implementation of Dynamic TOPMODEL and demonstrated its stable response to a range of spatial and temporal resolutions in simple catchments. The enhancements described provide much improved usability and interoperability with external data in portable formats. Distribution through the CRAN package mechanism will encourage the wider use of the model. The CRAN package includes all the information required to run an application to an agricultural catchment in the UK of around 10km² in size. This displays much more variability in land use and vegetation cover than the Gwy catchment, but the model performed satisfactorily against observed data with only minimal calibration.

Here we have concentrating on exploring the numerical characteristics of the model. This revealed that while the original implementation of Dynamic TOPMODEL made use of an implicit time stepping scheme for each HRU derived from a kinematic wave analogy, the implementation of this method was not fully implicit because the flows from "upslope" were only estimated at the start of the iteration. Explicit schemes for root and unsaturated zone moisture accounting remain and may be improved in the future. Thus the tests in this paper show that the predicted discharges are sensitive to both the time and space discretisations, but converge as the internal time step is reduced and the number of downslope HRUs increase. This concurs with Clark and Kavetskis' (2010) conclusion that the use of coarse time resolutions and spatial discretisations will have an impact on the parameter values required for the model to give an acceptable fit to observations.

Further developments will investigate applications of the model to more complex and heterogeneous basins in order to test the model's ability to simplify the system representation whilst retaining the key aspects of its dynamics and spatial variability. Testing of the channel routing algorithm for larger catchments, and improvements to the simple representation of the unsaturated zone while not increasing the number of parameters, would be valuable. The run-time performance of the model in its current implementation for the multiple realisations required for model calibration and uncertainty estimation is still an issue, but could be improved at the cost of losing some flexibility.

The simpler TOPMODEL code has been used in many different countries of the world, including applications where the basic assumptions are clearly violated. Dynamic TOPMODEL relaxes some of those assumptions whilst retaining many of the advantages of the original model. It is hoped that the guidance given in this paper about the sensitivities of the outputs to time and space discretisations will provide a useful guide to further applications in future.

Acknowledgments

This work has been funded by the JBA Trust (www.jbatrust.org) and managed by the Centre for Global Eco-innovation (CGE project number 132). A fully worked case study with example data and results will be developed and made available on request from the JBA Trust.

Many thanks to Wouter Buytaert, joint maintainer of the R-hydro project (https://r-forge.r-project.org/projects/r-hydro/), for his advice and encouragement in the use of R for hydrological modelling.

Source code, documentation and example data are available for download from the CRAN archive at http://cran.r-project.org/web/packages/dynatopmodel/index.html

7 Appendix: flux calculations in Dynamic TOPMODEL

Note: element-wise vector multiplication of vectors $\underline{q_1}$ and $\underline{q_2}$ is identical to multiplication of diagonal matrices $diag(\underline{q_1})$ and $diag(\underline{q_2})$ with leading elements equal to the corresponding vectors. This will be written as $\underline{q_1} * \underline{q_2}$

Similarly, element wise division of vectors is written as $\underline{q_1}/\underline{q_2} = \underline{q_3} * \underline{q_1}$, where $\underline{q_3} = diag(1/\underline{q_2})$

7.1 Root and unsaturated zone flux calculations

Actual evapotranspiration out of unsaturated areas, E_a [L], is calculated using a common formulation that minimises parametric demands (Beven, 2012)

$$E_a = E_p \frac{s_{rz}}{s_{rz,max}}$$

E_p is the potential evapotranspiration s_{rz} the root zone storage and $s_{rz,max}$ the maximum capacity .

Drainage flux q_{uz}into the water table from the unsaturated zone is calculated as:

$$q_{uz} = \frac{s_{uz}}{d.\, t_d} \qquad (1)$$

Where s_{uz} is the unsaturated storage for each group, d the specific storage deficits, and t_d ([T]/[L]) a time delay parameter reflecting the effective permeability of the soil across each unit.

7.2 Initialisation of subsurface state

Assuming that discharge results only from subsurface flow, that is, ignoring outputs via the root zone or saturation excess flow, total output from each unit is the specific base flow multiplied by the plan area $\underline{a}$:

$$\underline{Q_b} = \underline{a} * \underline{q_b}$$

Subsurface lateral input from upslope areas can be estimated from base flows redistributed by the flux distribution matrix:

$$\underline{Q_{in}} = \boldsymbol{W}^T \underline{Q_b}$$

Assuming steady specific river discharge of q_0, recharge to the water table by unsaturated gravity drainage must also equal q_0. Rain recharge will be reduced by any evapotranspiration but will be assumed sufficient to provide the required precipitation excess. Scaling up by the units' plan areas A gives the total vertical flux within each:

$$\underline{Q_{uz}} = q_0\, \underline{a}$$

Equating inputs and outputs across all HRUs

$$\underline{Q_{uz}} + \boldsymbol{W}^T \underline{Q_b} = \underline{Q_b}$$

$$\Longrightarrow (\boldsymbol{I} - \boldsymbol{W}^T)\underline{Q_b} = \underline{Q_{uz}}$$

$$\underline{Q_b} = (\boldsymbol{I} - \boldsymbol{W}^T)^{-1}\underline{Q_{uz}}$$

, where $\boldsymbol{I}$ is the identity matrix. The inverse to $(\boldsymbol{I} - \boldsymbol{W}^T)$, if one exists, and a solution for the initial base flows can be found with the `solve` method in R.

Denoting these flows converted back to specific discharges as $\underline{q_b}$, it can be shown (Beven, 2012) that an estimate for the corresponding initial average saturated storage deficits is

$$\overline{D}_0 = -mln\left(\bar{q}/\underline{q_b}\right)$$

, m being is the exponential recession parameter and $\bar{q} = e^{-\gamma}$, where γ is the areal average across the unit of the soil topographic index (Beven, 1986a), given by

$$\gamma = \frac{1}{A}\sum_{i}^{n} A_i ln(\frac{a}{T_0 tan(\beta)}) \qquad (2)$$

A_i is the area of each grid cell or partial cell comprising the area and A its total area.

The corresponding unsaturated zone drainage may be estimated by substituting $\overline{D}_0$ and q_0 into (1) and solving for q_{uz}

7.3 Subsurface routing

In the subsurface, mass continuity with storage (expressed as storage deficit, D) as the conserved variable and x in the downslope direction can be expressed as:

$$\frac{\partial D}{\partial t} = \frac{\partial q}{\partial x} - q_{uz}$$

q_{uz} is recharge from the unsaturated zone due to gravity drainage and q the specific subsurface flux in the downslope direction. Li *et al*. (1975) suggested that using q rather than D as the dependent variable would be more likely to result in convergence in a numeric scheme to solve for the time-varying quantities. Hence, incorporating the functional dependence of discharge on storage, the kinematic formulation for the flux is:

$$\frac{\partial q}{\partial t} = -c\frac{\partial q}{\partial x} + cr$$

$c = \frac{dq}{dD}$ is the downslope speed of propagation of a change in subsurface storage and is referred to as the kinematic wave velocity. With the exponential transmissivity profile adopted by TOPMODEL it can be shown that c is directly proportional to q, but other transmissivity profiles may be implemented within this framework.

Writing the average specific storage deficit for the response units at time t as the vector $\underline{D}$

$$\frac{d\underline{D}}{dt} = \underline{q_b} - \underline{q_{in}} - \underline{r} \qquad (3)$$

Where $\underline{r}$ is the recharge for each unit from the unsaturated zone, assumed constant over the time step. Applying the flow distribution matrix to $\underline{q_b}$ to obtain $\underline{q_{in}}$ gives an expression in $\underline{q} = \underline{q_b}$

$$\frac{d\underline{D}}{dt} = \underline{q} - \left(\boldsymbol{W}^T\, \underline{a} * \underline{q}\right) / \underline{a} - \underline{r} \tag{4}$$

Note that $\underline{q}_{in}$ has been divided by the units' areas, $\underline{a}$,

Given the exponential transmissivity profile adopted in Dynamic TOPMODEL, it can be shown that

$$\frac{d\underline{q}}{dt} = \frac{d\underline{q}}{d\underline{D}} \frac{d\underline{D}}{dt} = -\frac{\underline{q}}{\underline{m}} \frac{d\underline{D}}{dt} \tag{5}$$

Where the $\underline{m}$ are the exponential coefficients for the corresponding HRUs. Substitution gives:

$$\frac{d\underline{q}}{dt} = -\frac{\underline{q}}{\underline{m}} * \left(\underline{q} - \left(\boldsymbol{W}^T\, \underline{a} * \underline{q}\right) / \underline{a} - \underline{r}\right)$$

$$\frac{d\underline{q}}{dt} = \frac{\underline{q}}{\underline{m}} * \left(\boldsymbol{A}\underline{q} + \underline{r}\right) \tag{6}$$

With $\boldsymbol{A} = diag\left(\frac{1}{\underline{a}}\right) \boldsymbol{W}^T diag(\underline{a}) - \boldsymbol{I}$

Supplying the base flow at the previous step as the initial conditions, the system of non-linear ODEs given in (6) can be solved using a standard numerical approach to give an estimate for $\underline{q}(t)$. The programme employs the `lsoda` algorithm (Livermore Solver for Ordinary Differential Equations, Petzold and Hindmarsh, 1983) accessed via the `deSolve` package (Seibert *et al.*, 2010). It automatically selects the approach most suitable for the system supplied. For "non-stiff" systems it employs an explicit predictor-corrector solution, whereas for "stiff" systems an implicit backwards differentiation formula (BDF) is used. The algorithm is found in ODEPACK (Hindmarsh, 1983) and it, and its FORTRAN source, are available from NetLib http://www.netlib.org

7.4 Overland flow routing

If storage deficit predicted by the model falls below zero within any of the response units, excess storage and further input into that unit during the remainder of the time step is routed to a saturated excess store. After subsurface fluxes and storages have been updated, the surface excess of all HRUs is redistributed as overland flow into downslope units. Overland flow entering channel units (usually HRU#1) is routed to the outlet as for redistributed subsurface flow. Updated surface storage remaining on the land HRU is reallocated to the rainfall input of the corresponding units for the next time step, and the store emptied.

Any surface excess is assumed to be distributed evenly across the area of each unit. Given a vector of specific surface excess storages $\underline{s}$, and assuming a small storage depth so that non-linearity is minimised, surface flows out of the units are then

$$\underline{q}_{out} = \underline{v} * \underline{s} \tag{7}$$

The elements of $\underline{v}$ are the fixed overland flow velocities supplied for each HRU. These may vary according to surface roughness and slope and be determined, for example, by supplying a Manning *n* value and average gradient within

each unit. Surface flow is now distributed downslope between units in the same proportions as for the subsurface. The vector of input flux from upslope units is therefore

$$q_{in} = \boldsymbol{A}\underline{q} \tag{8}$$

, with $\boldsymbol{A}$ as previously defined. Combining (7) and (8) results in a system of linear ordinary differential equations for $\underline{s}$ in terms of time *t*:

$$\frac{d\underline{s}}{dt} = \boldsymbol{A}\underline{v} * \underline{s} - \underline{v} * \underline{s} = \boldsymbol{A}'\underline{s} \tag{9}$$

, with $\boldsymbol{A}' = \underline{v} * (\boldsymbol{A} - \boldsymbol{I})$

This system may be solved by the Eigenvalue Method outlined by Dummit (2012). It can be shown that the general solution to (9) is

$$\underline{s}(t) = \sum_{i=1}^{n} c_i e^{\lambda_i t} \underline{u_i} \tag{10}$$

Where $\underline{u_i}$ are the eigenvectors of $\boldsymbol{A}'$, λ_i the corresponding eigenvalues and c_i are arbitrary constants to be determined by any boundary conditions. Substituting the HRU surface storages $\underline{s}(0)$ at *t=0*, gives a system of simultaneous equation for the coefficients. Setting $\boldsymbol{U}$ to be a matrix whose columns comprise the eigenvectors of $\boldsymbol{A}'$, and $\underline{c} = \begin{pmatrix} c_1 \\ c_2 \\ \vdots \\ c_n \end{pmatrix}$ the system can be written as $\boldsymbol{U}\underline{c} = \underline{s}(0)$. Therefore:

$$\underline{c} = \boldsymbol{U}^{-1}\underline{s}(0) \tag{11}$$

A solution to (11) is easily obtained using the R `solve` method, for instance. Substitution back into (10) allows the overland storage across a time step to be calculated, and division by length of time step supplies the specific overland flow rate across the interval.

Given overland flow velocities fixed across a simulation period, the eigenmatrix $\boldsymbol{U}$ and eigenvalues may be pre-calculated so that in the above method just the solution to (11) will require intensive computation. As `solve` makes use of the LAPACK compiled library (see Anderson *et al.*, 1999), this stage is however extremely fast.

7.5 Determination of maximum subsurface flow

Storm flow routed from upslope areas that exceeds a downslope unit's subsurface throughput capacity will return to the surface as base flow excess. The programme identifies this situation and the capacity at which base flow excess starts is calculated for each unit at the start of a programme run.

Beven (2012) gives an expression for the base flow out of a catchment area as

$$Q_b = Q_0 e^{-\overline{D}/m} \tag{12}$$

with $$Q_0 = Ae^{-\gamma}$$

$\overline{D}$ is the average storage deficit and γ is as defined in (2). Assuming limiting transmissivity is constant within the HRU, $\gamma = ln(T_0) - \lambda$ with $\lambda = \frac{1}{A}\sum_i^n A_i ln(\frac{a}{tan(\beta)})$ a constant for the response unit that may therefore be calculated in the pre-processing module and supplied as a run-time parameter. Setting $\overline{D} = 0$ in (12) the maximum specific base flow from a unit is seen to be

$$q_{max} = e^{-\gamma} = \frac{T_0}{e^{\lambda}} \qquad (13)$$

Clearly not all elements within a HRU share the same topography but (13) provides a constraint on its total downslope flow and indicates when some areas will start to generate base flow excess overland flow. Larger values of limiting transmissivity indicate a higher potential subsurface flow. Flat or convergent topography or areas far downslope will saturate relatively more frequently, as is observed in the field.

References

Anderson. E. and ten others (1999) LAPACK Users' Guide. Third Edition. SIAM. Available on-line at http://www.netlib.org/lapack/lug/lapack_lug.html.

Andrews, F. T., Croke, B. F. W., & Jakeman, A. J. (2011). An open software environment for hydrological model assessment and development. Environmental Modelling & Software, 26, 1171-1185. doi:10.1016/j.envsoft.2011.04.006

Barling, R. D., Moore, I. D., & Grayson, R. B. (1994). A quasi-dynamic wetness index for characterizing the spatial distribution of zones of surface saturation and soil water content. Water Resources Research, 30(4), 1029-1044.

Bashford, K. E., Beven, K. J. and Young, P C, 2002, Observational data and scale dependent parameterisations: explorations using a virtual hydrological reality, Hydrol. Process.,16(2), 293-312.

Beven, K.J. (1979), 'On the generalised kinematic routing method'. Water Resour. Res., 15(5), 1238-1242.

Beven, K. (1981). Kinematic subsurface stormflow. Water Resour. Res., 17(5), 1419-1424

Beven, K. (1986a). Runoff production and flood frequency in catchments of order *n*: an alternative approach. V.K. Gupta, I. Rodriguez-Iturbe, E.F. Wood (Eds.), Scale Problems in Hydrology, D. Reidel, Dordrecht (1986), pp. 107‑131

Beven, K. (1989). TOPMODEL: a critque, *Hydrol. Process.*, 11(9), 1069-1086

Beven, K. (2000), On the future of distributed modelling in hydrology. Hydrol. Process., 14: 3183–3184. doi: 10.1002/1099-1085(200011/12)14:16/17<3183::AID-HYP404>3.0.CO;2-K

Beven, K. (1993). Prophecy, reality and uncertainty in distributed hydrological modelling. Adv. Water Resour., 16(1), 41-51.

Beven, K. (2002). Towards a coherent philosophy for modelling the environment.Proceedings of the Royal Society of London. Series A: 458(2026), 2465-2484.

Beven, K. (2012). Rainfall-*Runoff Modelling*: the *Primer*. Wiley-Blackwell: Chichester

Beven, K J, Cloke, H., Pappenberger, F, Lamb, R and Hunter, N, 2015. Hyperresolution information and hyperresolution ignorance in modelling the hydrology of the land surface. SCIENCE CHINA Earth Sciences, 58 (1): 25-35.

Beven, K., & Freer, J. (2001b). Equifinality, data assimilation, and uncertainty estimation in mechanistic modelling of complex environmental systems using the GLUE methodology. Journal of Hydrology, 249(1), 11-29.

Beven, K. and Kirkby, M. (1979). A physically based variable contributing area model of basin hydrology. Hydrol. Sci. Bull 24(1): 43-69.

Beven, K., Lamb, R., Quinn, P., Romanowicz, R., and Freer, J. (1995). Topmodel. In V. P. Singh (Ed.) *Computer Models* of *Watershed Hydrology*, Water Resource Publications, CO, 627-668.

Beven, K., P. Smith, I. Westerberg, and J. Freer (2012), Comment on ‘‘Pursuing the method of multiple working hypotheses for hydrological modeling’’ by M. P. Clark et al., Water Resour. Res., 48, W11801, doi:10.1029/2012WR012282.

Beven, K. J., and Smith, P. J., 2014, Concepts of Information Content and Likelihood in Parameter Calibration for Hydrological Simulation Models, ASCE J. Hydrol. Eng., DOI: 10.1061/(ASCE)HE.1943-5584.0000991.

Beven, K., & Wood, E. F. (1983). Catchment geomorphology and the dynamics of runoff contributing areas. Journal of Hydrology, 65(1–3), 139-158. doi: http://dx.doi.org/10.1016/0022-1694(83)90214-7

Bivand, R. (2014). `spgrass6`: Interface between GRASS 6 and R. R package version 0.8-6. http://CRAN.R-project.org/package=spgrass6

Bivand, R. & Rundel, C. (2014). `rgeos`: Interface to Geometry Engine - Open Source (GEOS). R package version 0.3-4. http://CRAN.R-project.org/package=rgeos

Bivand, R. Keitt, T. & Rowlingson, B. (2014). `rgdal`: Bindings for the Geospatial Data Abstraction Library. R package version 0.8-16. http://CRAN.R-project.org/package=rgdal

Buytaert, W., Reusser, D., Krause, S., & Renaud, J.-P. (2008). Why can't we do better than Topmodel? Hydrological Processes, 22, 4175-4179.

Buytaert, W. (2011). `topmodel`: Implementation of the hydrological model TOPMODEL in R. R package version 0.7.2-2. http://CRAN.R-project.org/package=topmodel

Clark, M. P., and D. Kavetski (2010), Ancient numerical daemons of conceptual hydrological modeling: 1. Fidelity and efficiency of time stepping schemes, Water Resour. Res.,46, W10510, doi:10.1029/2009WR008894.

Dowle, M., Short, T., Lianoglou, S., Srinivasan, A. with contributions from R Saporta and E Antonyan (2014). `data.table`: Extension of data.frame. R package version 1.9.4. http://CRAN.R-project.org/package=data.table

Dummit, E (2012). Differential Equations (part 3): Systems of First-Order Differential Equations. Downloaded 16/01/2015 from http://www.math.wisc.edu/~dummit/docs/diffeq_3_systems_of_linear_diffeq.pdf

Freer, J., K. J. Beven, and N. E. Peters (2003), Multivariate seasonal period model rejection within the generalised likelihood uncertainty estimation procedure, in *Calibration of Watershed Models*, edited by Q. Duan, H. Gupta, S. Sorooshian, A. N. Rousseau and R. Turcotte, pp. 69-88, AGU, Water Science and Application Series, Washington.

Freer, J. E., McMillan, H., McDonnell, J. J., & Beven, K. J. (2004). Constraining dynamic TOPMODEL responses for imprecise water table information using fuzzy rule based performance measures. Journal of Hydrology, 291(3), 254-277.

Furrer, R., Sain, S. (2010). `spam`: A Sparse Matrix R Package with Emphasis on MCMC Methods for Gaussian Markov Random Fields. Journal of Statistical Software, 36(10), 1-25. URL http://www.jstatsoft.org/v36/i10/.

Gilman, K., & Newson, M. D. (1980). Soil pipes and pipeflow. A hydrological study in upland Wales. Geobooks: Norwich.

Hijmans, R (2014). `raster`: Geographic data analysis and modeling. R package version 2.2-31. http://CRAN.R-project.org/package=raster

Hindmarsh, Alan C. (1983) `ODEPACK`, A Systematized Collection of ODE Solvers; in p.55–64 of Stepleman, R.W. et al.[ed.] (1983) *Scientific Computing*, North-Holland, Amsterdam.

Jakeman, A. J., and G. M. Hornberger (1993), How much complexity is warranted in a rainfall-runoff model?, Water Resour. Res., 29(8), 2637–2649, doi:10.1029/93WR00877.

Jencso, K. G., McGlynn, B. L., Gooseff, M. N., Wondzell, S. M., Bencala, K. E., & Marshall, L. A. (2009). Hydrologic connectivity between landscapes and streams: Transferring reach-and plot-scale understanding to the catchment scale. Water Resour. Res., 45(4): W04428, DOI: 10.1029/2008WR007225

Jones, J. A. A. (2010). Soil piping and catchment response. Hydrological processes, 24(12), 1548-1566.

Keitt, T. H., Bivand, R., Pebesma, E., & Rowlingson, B. (2011). `rgdal`: bindings for the Geospatial Data Abstraction Library. R package version 0.7-1, URL http://CRAN. R-project. org/package= rgdal.

Lane, S. N., Brookes, C. J., Kirkby, M. J., & Holden, J. (2004). A network-index-based version of TOPMODEL for use with high-resolution digital topographic data. Hydrological Processes, 18(1), 191-201.

Liu, Y, Freer, JE, Beven, KJ and Matgen, P, 2009, Towards a limits of acceptability approach to the calibration of hydrological models: extending observation error, J. Hydrol., 367:93-103, doi:10.1016/j.jhydrol.2009.01.016.

McDonnell, J. J., Sivapalan, M., Vaché, K., Dunn, S., Grant, G., Haggerty, R., ... & Weiler, M. (2007). Moving beyond heterogeneity and process complexity: A new vision for watershed hydrology. Water Resour. Res., 43, W07301, doi:10.1029/2006WR005467.

McGuire, K. J., & McDonnell, J. J. (2010). Hydrological connectivity of hillslopes and streams: Characteristic time scales and nonlinearities. Water Resources Research, 46(10): W10543 DOI: 10.1029/2010WR009341

McNeil, D. D. (1997). Direct measurement of evaporation from grassland at Plynlimon. Hydrology and Earth System Sciences Discussions, 1(3), 447-452

Marc, V., & Robinson, M. (2007). The long-term water balance (1972–2004) of upland forestry and grassland at Plynlimon, mid-Wales. Hydrology and Earth System Sciences, 11(1), 44-60.

Newson, A. J. (1976a). Some aspects of the rainfall of Plynlimon, mid-Wales. Report No. 30. Wallingford: Institute of Hydrology.

Newson, M. D. (1976b). The physiography, deposits and vegetation of the Plynlimon catchments.(A synthesis of published work and initial findings).Report No. 34. Wallingford: Institute of Hydrology.

Newson, M. D., & Gilman, K. (Eds.). (1991). Plynlimon research: the first two decades (p. 188). Wallingford: Institute of Hydrology.

Page, T., Beven, K. J., Freer, J., & Neal, C. (2007). Modelling the chloride signal at Plynlimon, Wales, using a modified dynamic TOPMODEL incorporating conservative chemical mixing (with uncertainty). Hydrological Processes, 21(3), 292-307.

Petzold, L. (1983) Automatic Selection of Methods for Solving Stiff and Nonstiff Systems of Ordinary Differential Equations. Siam J. Sci. Stat. Comput. 4, 136–148.

PROFILE DTM [DXF geospatial data], Scale 1:10000, Tiles: sn89sw,sn89se,sn88sw,sn88nw,sn88ne,sn88se,sn78ne,sn78se,sn79se, Updated: November 2009, Ordnance Survey (GB), Using: EDINA Digimap Ordnance Survey Service, <http://edina.ac.uk/digimap>, Downloaded: Thu Jul 04 17:24:10 GMT 2013

Peters, N. E., J. Freer, and K. Beven (2003), Modelling hydrologic responses in a small forested catchment (Panola Mountain, Georgia, USA): a comparison of the original and a new dynamic TOPMODEL, Hydrological Processes, 17(2), 345-362.

Quinn, P., K.J. Beven and A. Culf (1995), The introduction of macroscale hydrological complexity into land surface-atmosphere transfer models and the effect of planetary boundary layer development, Journal of Hydrology, 166, 421-444.

R Core Team (2013). R: A language and environment for statistical computing. R Foundation for Statistical Computing, Vienna, Austria. ISBN 3-900051-07-0, URL http://www.R-project.org/.

Ryan, J. A., & Ulrich, J. M. (2008). `xts`: Extensible Time Series. R package version 0.0-5, URL http://CRAN. R-project. org/package= xts.

Soetaert, K., Petzoldt, T & Woodrow Setzer, R. (2010). Solving Differential Equations in R: Package `deSolve` Journal of Statistical Software, 33(9), 1--25. URL http://www.jstatsoft.org/v33/i09/.

Tarboton, DG, 1997, A new method for the determination of flow directions and upslope areas in grid digital elevation models, Water Resources Research, 33(2): 309-319 DOI: 10.1029/96WR03137

Wigmosta, M. S., & Lettenmaier, D. P. (1999). A comparison of simplified methods for routing topographically driven subsurface flow. *Water Resources Research*, *35*(1), 255-264.

Younger, P. M., Gadian, A. M., Wang, C. G., Freer, J. E., & Beven, K. J. (2008). The usability of 250 m resolution data from the UK Meteorological Office Unified Model as input data for a hydrological model. Meteorological Applications, 15(2), 207-217.

Younger, P. M., Freer, J. E., & Beven, K. J. (2009). Detecting the effects of spatial variability of rainfall on hydrological modelling within an uncertainty analysis framework. Hydrological Processes, 23(14), 1988-2003.

Zeileis, A., & Grothendieck, G. (2005). `zoo`: S3 infrastructure for regular and irregular time series. Journal of Statistical Software, 14(6), 1-27. URL http://www.jstatsoft.org/v14/i06/

Figures

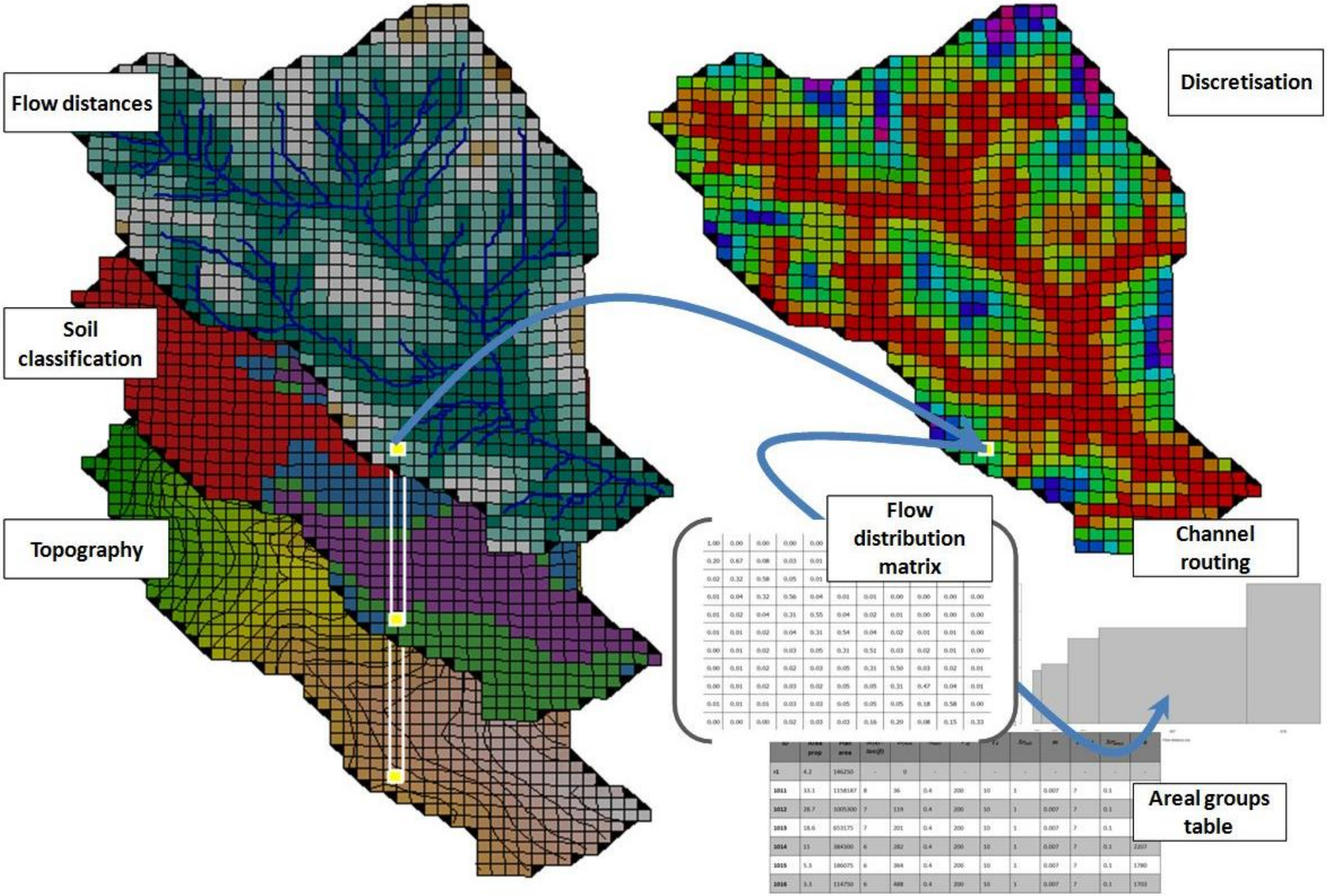

Figure 1. Aggregation of landscape layers into a catchment discretisation and its associated data structures

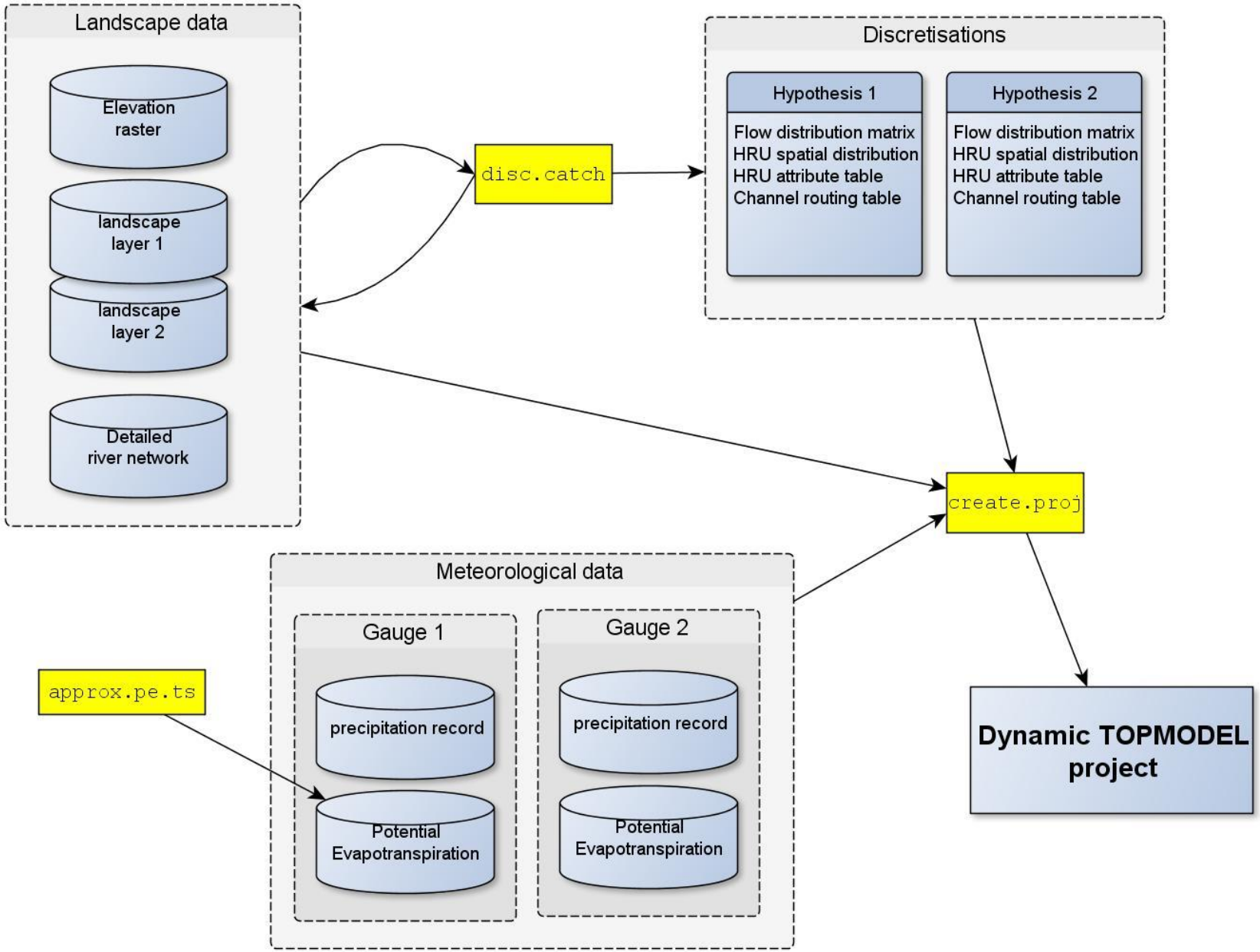

Figure 2. Dynamic TOPMODEL pre-processing workflow

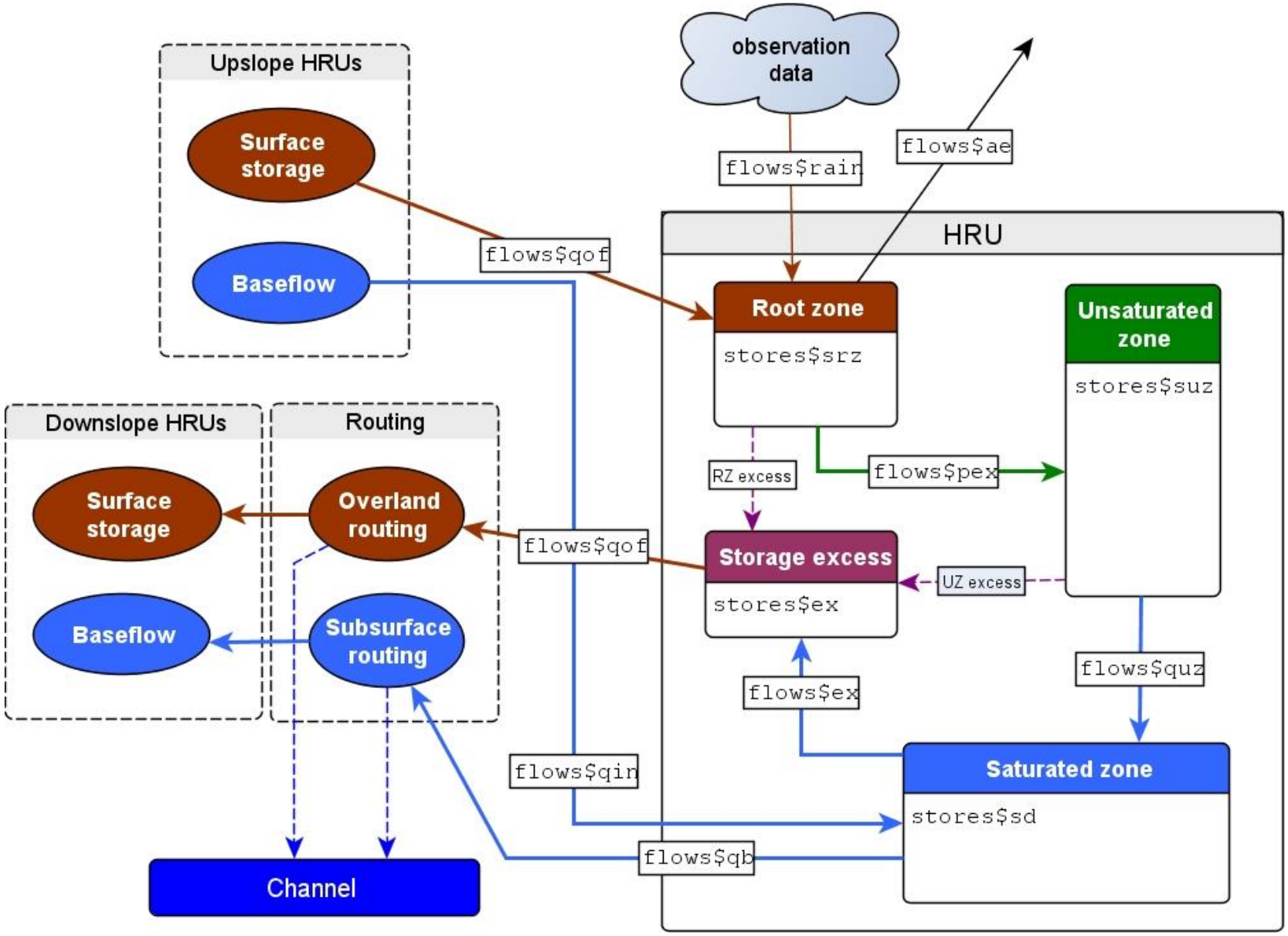

Figure 3. Conceptual structure and interfaces of hydrological response groups. Components map to the fields in tables 1 -3

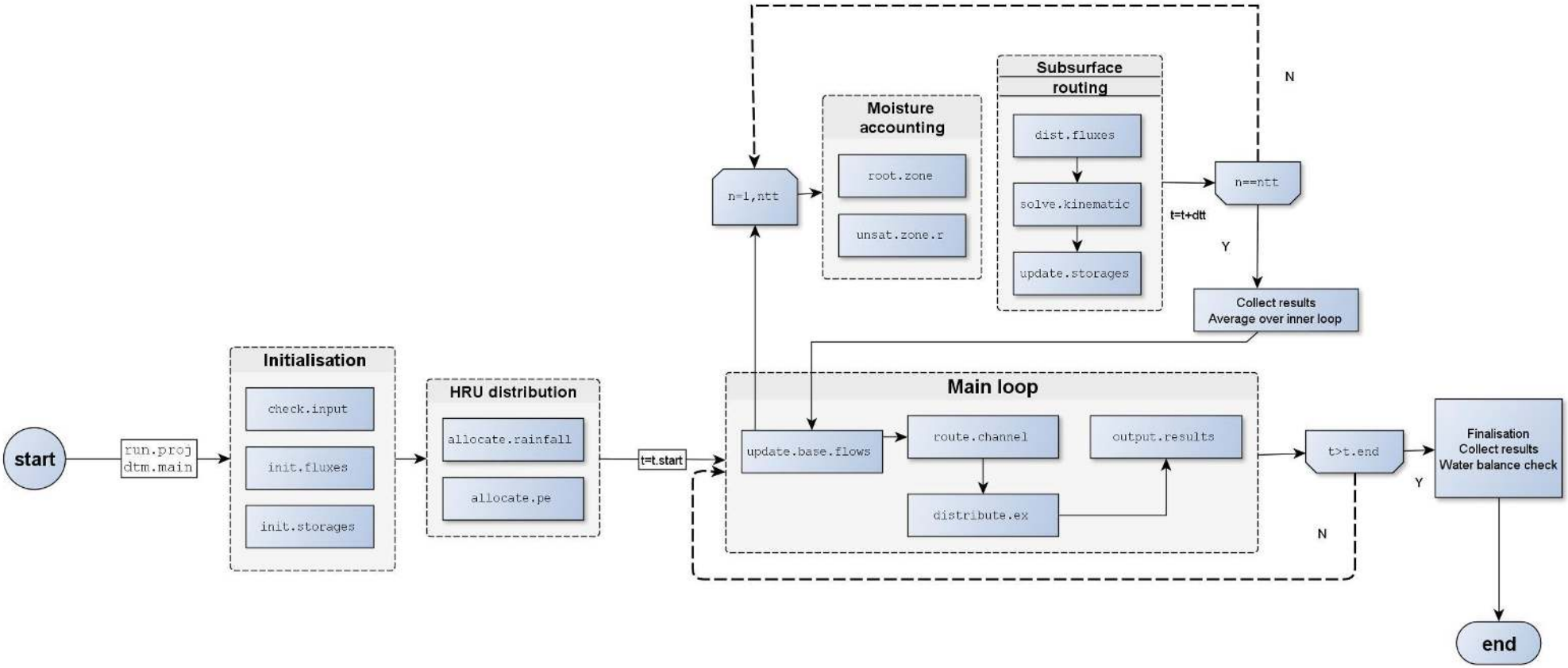

Figure 4. Dynamic TOPMODEL modular programme structure

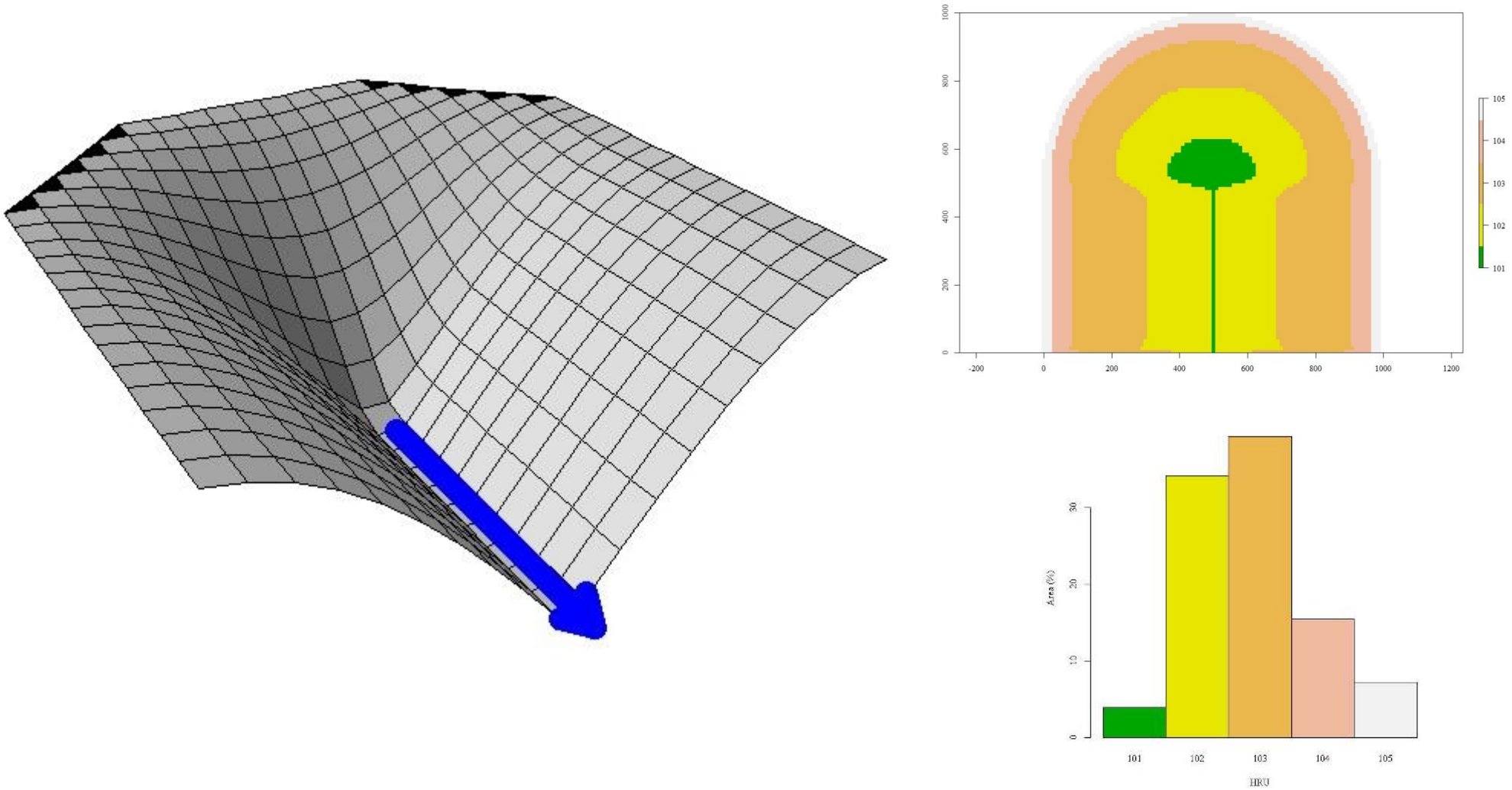

Figure 5: Simulated upland basin with a simple straight channel used in initial spatial and temporal sensitivity tests. Results are shown of an aggregation into 5 units according to upslope contributing area. Bar plots shows the plan areal contribution for each unit

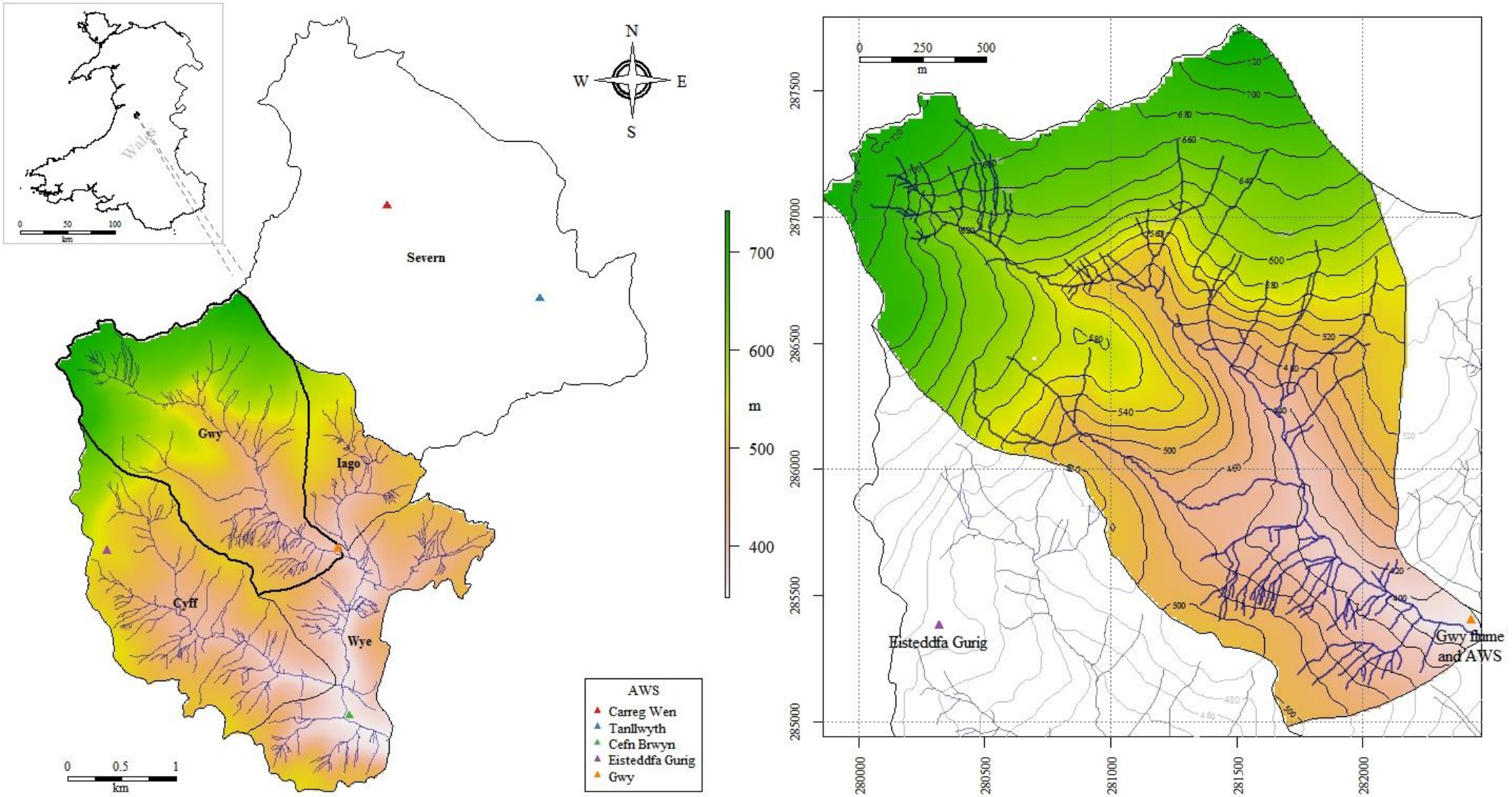

Figure 6: Overview of Gwy test basin, showing its location within the Plynlimon research catchments in mid Wales. The channel network for Wye and weather station locations are also shown. Digital elevation data ©Ordnance Survey (GB), 2012. Catchment boundaries and digital river network, CEH (2012)

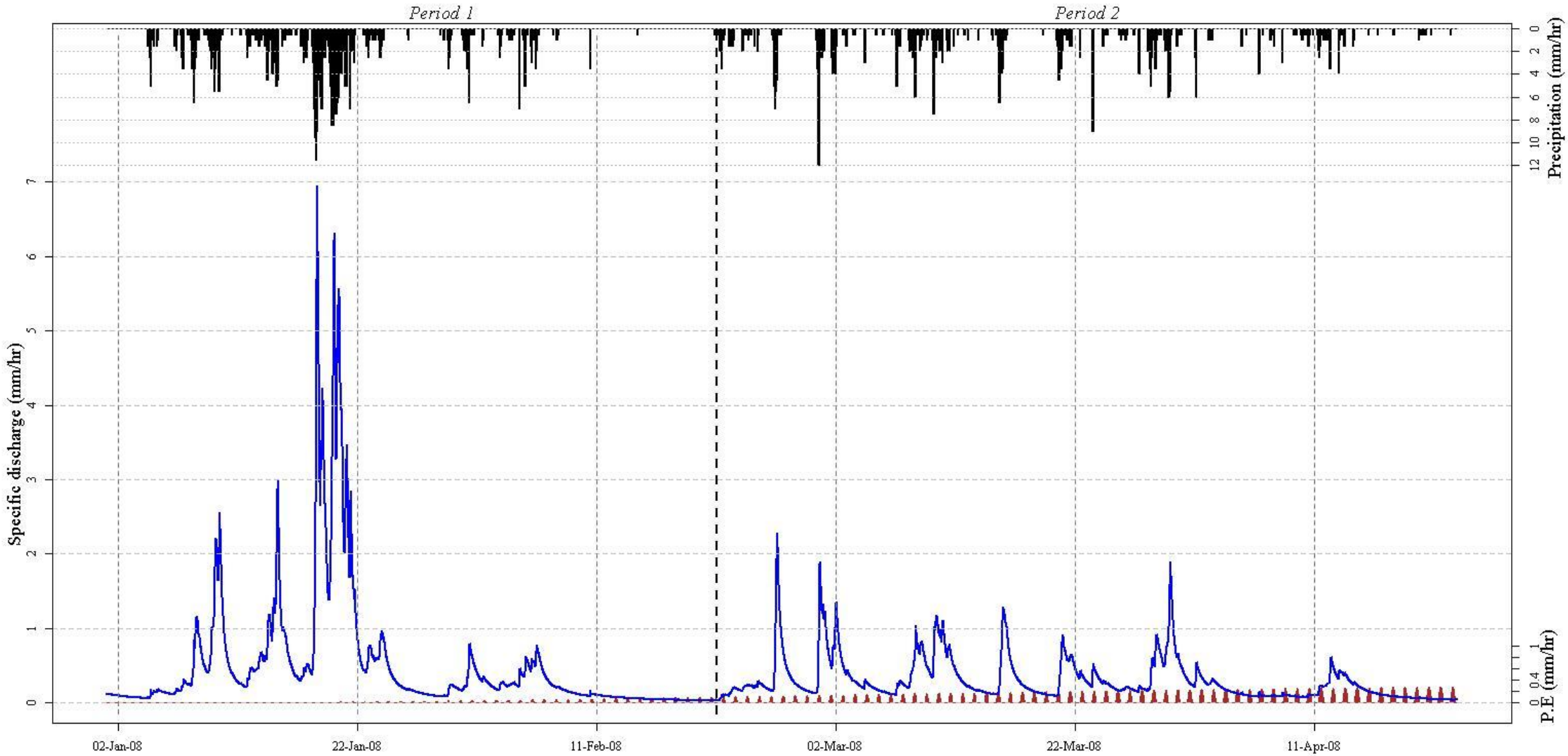

Figure 7: Test period showing rainfall, estimated potential evapotranspiration (in brown, simulated) and observed discharges at the Gwy flume. Storms occupy the first month of the simulation, separated by a week of dry weather from a period of less intense but persistent rainfall lasting from late February through to April. The dotted line marks the division between the two periods.

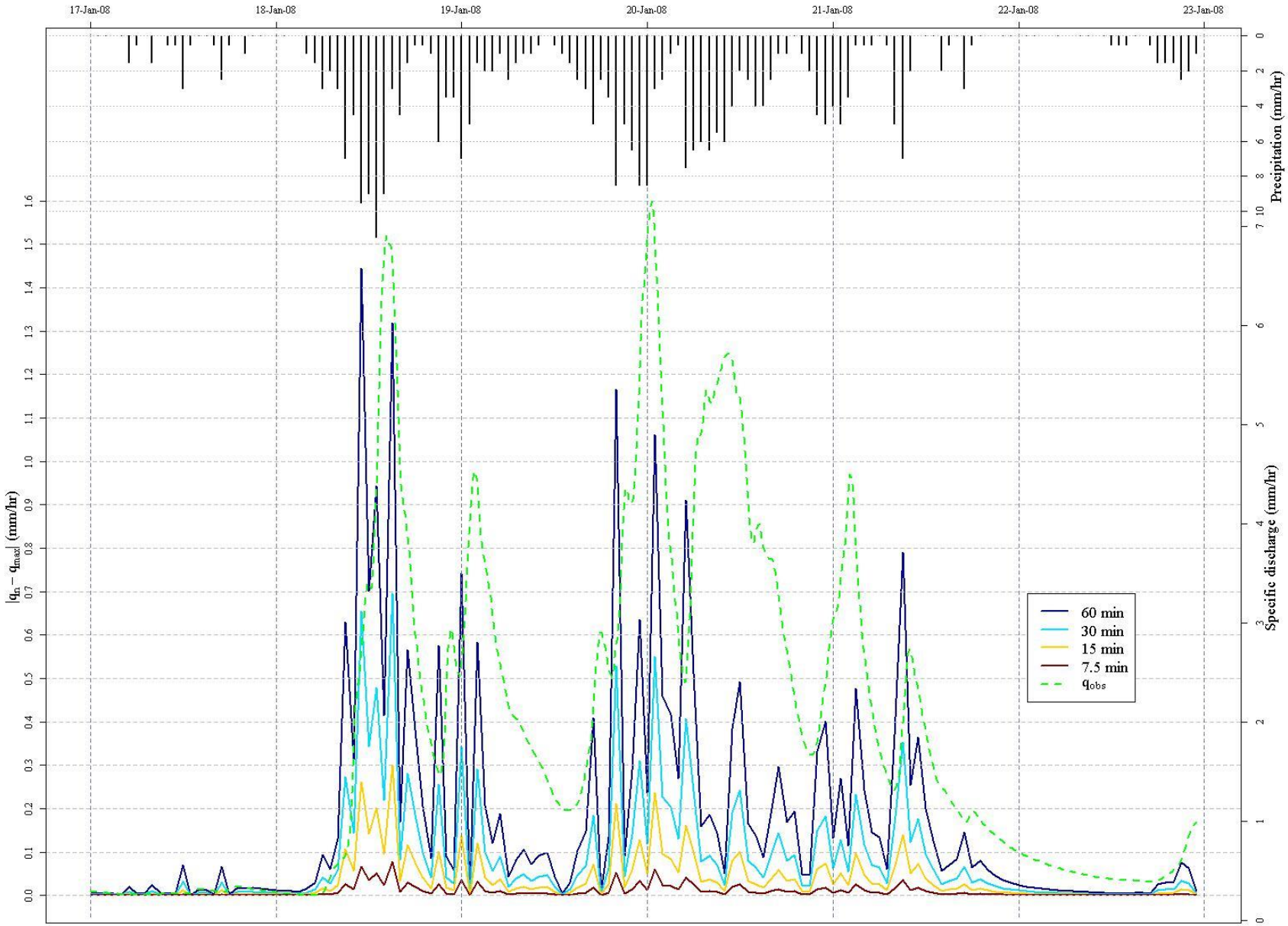

Figure 8. Response of hypothetical catchment to changes in time interval. Shown are the absolute difference of the predicted discharges within each trial from those predicted using a time step of 5 minutes. Central part of storm event within test period show and evapotranspiration output suppressed. Observed discharges are shown in green using the RH axis for scale.

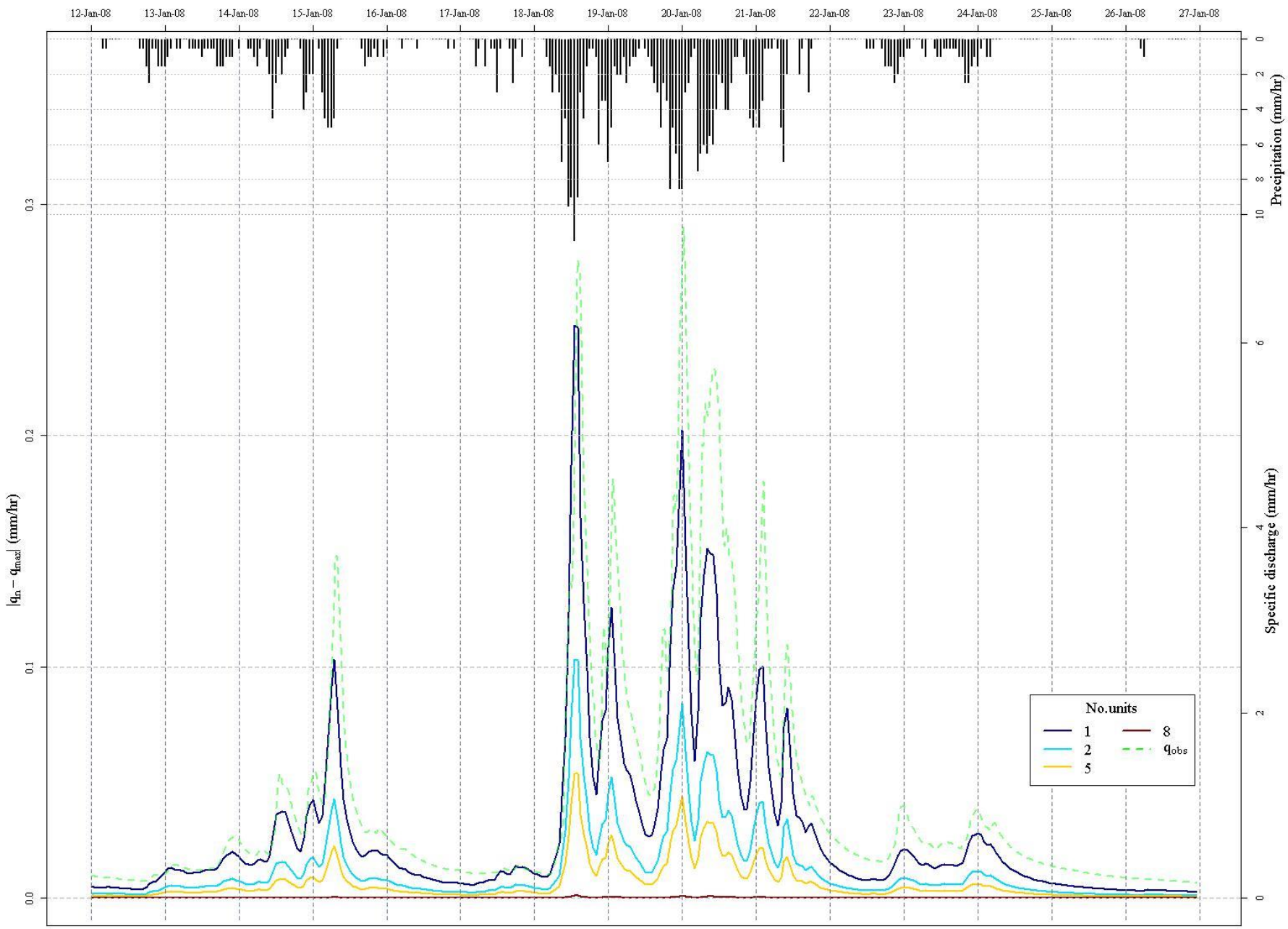

Figure 9. Response of hypothetical catchment to changes in spatial discretisation. Shown are the absolute difference of the predicted discharges within each trial from those predicted using a time step of 5 minutes. Central part of storm event within test period shown and evapotranspiration output suppressed. Observed discharges are shown in green

using the RH axis for scale.

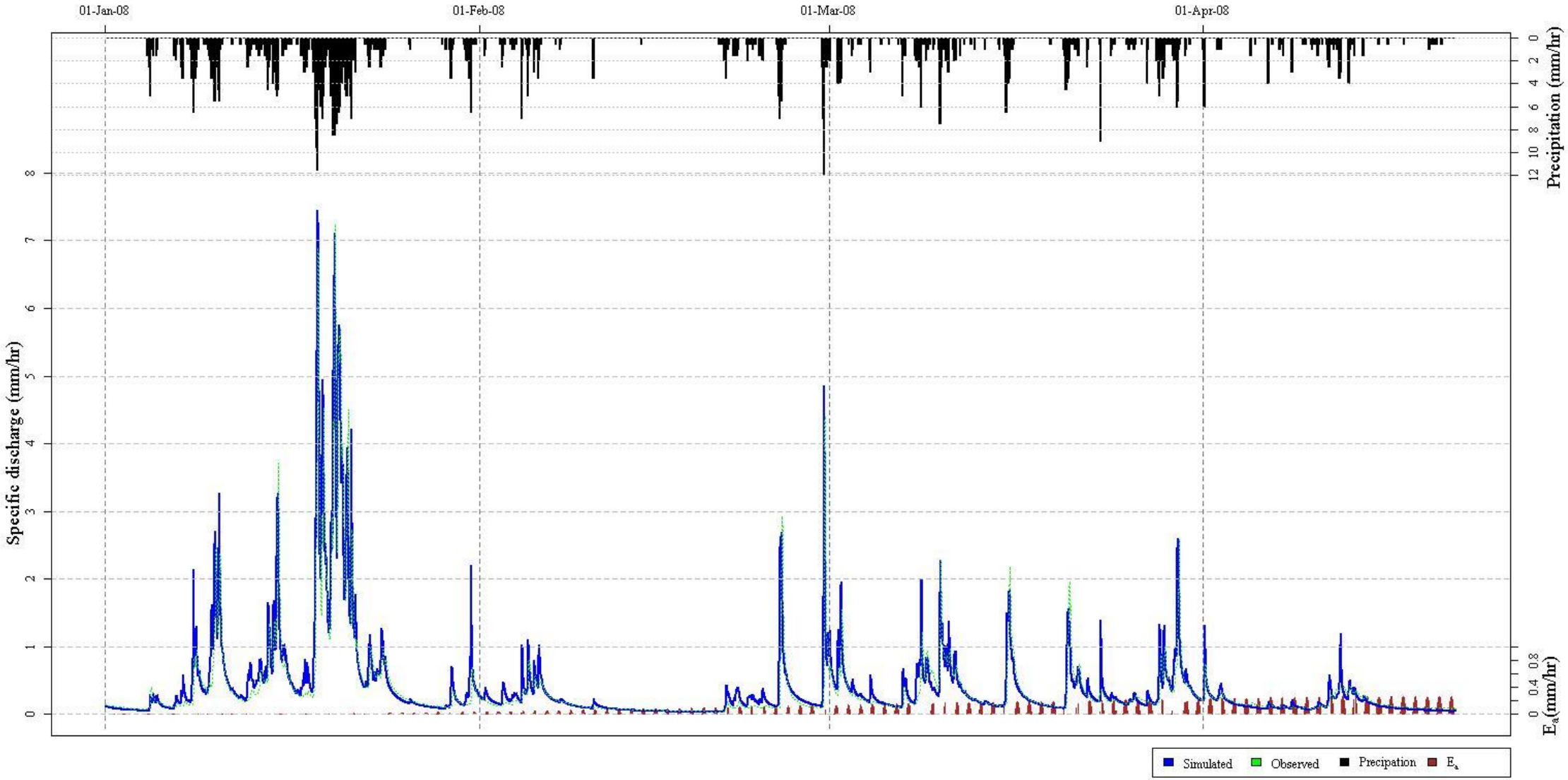

Figure 10: Four month validation period showing observed discharges (green) and simulated (blue) values for a run using a 15 minute time interval and 3 inner steps. Calculated actual evapotranspiration is shown in brown using the scale on the RH axis.